

MULTISCALE SPECTRAL AMG_E SOLVERS FOR HIGH-CONTRAST FLOW PROBLEMS

YALCHIN EFENDIEV, JUAN GALVIS, AND PANAYOT S. VASSILEVSKI

ABSTRACT. We construct and analyze multigrid methods with nested coarse spaces for second-order elliptic problems with high-contrast multiscale coefficients. The design of the methods utilizes stable multilevel decompositions with a bound that generally grows with the number of levels. To stabilize this growth, in our theory, we use AMLI-cycle multigrid which leads to an overall optimal cost algorithm. The robustness, with respect to the contrast, is guaranteed due to the combined effect of the Schwarz smoothers used and the spectral construction of the coarse bases. More specifically, in order to obtain an optimal multilevel decomposition, we combine multigrid ideas in the recent two-level methods in [Multiscale Model. Simul. 8(5), 1621-1644], and earlier, in the element-based algebraic multigrid methods (or AMG_E), that use local spectral problems to enrich the coarse space. In general, the intermediate coarse spaces need to be enriched in order to get contrast-independent convergence. The general techniques presented here allow us to study the problem of an optimal enrichment in the sense of enriching with a minimal number of extra coarse degrees of freedom. Thus, the methods we develop are optimal, with respect to both the contrast and the number of levels used. Moreover, we have the potential to achieve this goal with a minimal number of coarse degrees of freedom. We present numerical results that illustrate our theoretical findings.

1. INTRODUCTION

Multiscale phenomena occur in many applications such as flow in porous media, material sciences, and so on. In these applications, media properties vary at small scales and, moreover, the variation in the media properties can be very large. The latter brings an additional small-scale parameter represented as the ratio between the largest and smallest conductivity values. Iterative solvers for such multiscale problems are adversely affected by the contrast in the media properties when multiple scales are present within coarse regions. In two-level methods, with a careful choice of coarse regions, one can reduce the variations within coarse regions, while this is not the case for multilevel solvers. In multilevel solvers, one eventually encounters large variations within coarse partitions. These variations affect the performance of the solvers. The design of robust preconditioners, with contrast-independent performance, requires

Date: November 29, 2009–beginning; Today is January 27, 2012.

1991 Mathematics Subject Classification. 65F10, 65N20, 65N30.

Key words and phrases. coarse spaces, spectral element algebraic multigrid, multiscale PDEs, overlapping Schwarz method.

This work was performed under the auspices of the U.S. Department of Energy by Lawrence Livermore National Laboratory under Contract DE-AC52-07NA27344.

special coarse spaces. Our goal is to study coarse spaces that can provide contrast-independent multilevel preconditioners and have a minimal (or small) dimension.

The purpose of this paper is to study the performance of recently proposed overlapping Schwarz methods [5] for elliptic equations with high-contrast coefficients. These methods converge independently of the contrast and use a spectral construction of the coarse space. In this paper, we extend the methods and results of [5, 6, 7] to the multilevel case. We refer to [8] for a review of the results and techniques in [5, 6, 7]. In the earlier work [11], we presented some preliminary results and numerical test in this direction. In [11], we proposed two multilevel methods that extend the ideas of [5]. The first method is not genuinely multilevel in the sense that the fine grid has to be visited from every intermediate level in order to compute coarse basis functions. This results in high computational cost. Also, the resulting coarse spaces are not nested which makes the numerical and mathematical analysis more difficult. The second method proposed in [11] is a genuine multilevel method and the fine grid does not need to be visited in order to compute coarse basis functions. Some preliminary numerical studies were also presented. In the current paper, we design and analyze genuine multilevel methods in a more general setting. In particular, we extend the genuine multilevel method presented earlier in [11]. All multilevel methods that we construct in the present paper, are optimal in terms of the contrast. Our theory also allows the use of the more involved (than the V-cycle) AMLI-cycle MG which we prove can lead to an overall optimal MG method also with respect to the number of levels used (and to maintain contrast-independent bounds).

We note that the multilevel methods developed here are related to *spectral agglomerate algebraic multigrid* methods (or agglomerate ρ AMGe), proposed originally in [3] (see also [2]) and then extended in [4] to allow for multilevel recursion without visiting the fine level. A computational survey on various AMGe methods is found in [14]; see also [17]. The two-level approach proposed in [5] allows for pure “algebraic” implementation if used within an element agglomeration setting (for element agglomeration, cf., e.g., [14] or [17]). It needs only to identify the “vertices” of the agglomerates; no additional topological relations are required (assuming that we have somehow come up with an agglomeration algorithm or if geometric meshes are used). The methods introduced here differ from the previously proposed similar spectral agglomerate AMGe methods in [3, 4]. The difference occurs due to the fact that the present method uses overlapping subdomains (unions of fine grid agglomerates (elements) that share a common vertex) as domains where the local eigenproblems are posed. To define the resulting coarse basis, a partition of *identity* is applied at the end. To implement the method algebraically, we would need an agglomeration algorithm and an algorithm to generate the vertices of the resulting agglomerates at every level. Other topological relations are not needed. Also, there is no need to compute reduced Schur complements of local matrices (as in [4, 14]) and still the method allows for recursion without visiting the finest grid; see Section 5.1. Instead, an appropriate partition of *identity* needs to be constructed between any two consecutive levels, which is a key ingredient of the method. Its choice also has implications on the coarse space dimension.

According to [5, 6, 7, 8, 11, 13, 9], obtaining two-level methods that are optimal with respect to the contrast is a challenging task. Depending on the high-contrast coefficient, additional coarse degrees of freedom are generally required in the coarse problem. Identifying these additional degrees of freedom is important. In [5], motivated by weighted Poincaré inequalities, the authors propose a local generalized eigenvalue problem to identify the important degrees of freedom that one needs to include in the coarse problem. Moreover, [6, 8] explored the idea of selecting adequate eigenvalue problems leading to a minimal dimension coarse space; see Section 4.1. The idea is to use a judiciously chosen initial partition of *identity* to construct a modified weight for the local eigenvalue problem. The resulting two-level method uses a coarse space of optimal dimension and yields two level methods that are robust with respect to the contrast. In this paper, we design multilevel methods that extend the ideas presented in [5, 6, 7, 8, 9] for the construction of optimal enrichments. For the construction, we reformulate the two level methods in [6] in an algebraic way. A key ingredient in the construction is to replace the role of partition of *unity* functions by partition of *identity* operators. Using this algebraic setting, we are able to design robust multilevel methods. This extension to genuine multilevel methods is not straightforward, especially when the effects of high-conductivity regions on coarse spaces is different at two consecutive coarse grids. Our analysis shows that the bounds in the constructed multilevel space decomposition are contrast independent but generally grow with the number of levels. To stabilize this growth, our theory resorts (in Section 5.4) to the more involved (than the V-cycle) AMLI-cycle MG, which allows us to achieve both contrast-independent and level-independent MG convergence bounds.

The remainder of the paper is structured as follows. We present the model problem in Section 2. We demonstrate the main recursive construction in Section 3, where we design and analyze an abstract three-level method. In Section 4, we present some particular examples of our abstract construction. We introduce and analyze our MG algorithms in Section 5. Some remarks on the computational cost are presented in Section 6. Section 7 contains some numerical tests that validate our theoretical results. And in Section 8 we make some conclusions.

2. MODEL PROBLEM, MESHES AND COEFFICIENT DESCRIPTION

Let $D \subset \mathbb{R}^2$ (or \mathbb{R}^3) be a polygonal domain. We want to find $u^* \in H_0^1(D)$ such that

$$(2.1) \quad a(u^*, v) = f(v) \quad \text{for all } v \in H_0^1(D),$$

where the bilinear form a and the functional f are defined by

$$(2.2) \quad a(u, v) = \int_D \kappa(x) \nabla u(x) \cdot \nabla v(x)$$

and $f(v) = \int_D f(x)v(x)$ for all $u, v \in H_0^1(D)$. We allow discontinuous and high-contrast coefficient κ ; that is,

$$\eta := \frac{\max_{x \in D} \kappa(x)}{\min_{x \in D} \kappa(x)} \gg 1.$$

For the analysis, we assume that D is triangulated by \mathcal{L} meshes $\mathcal{T}^{(\ell)}$, $\ell = 0, \dots, \mathcal{L}$, which are a nested refinement of a coarse triangulation $\mathcal{T}_H = \mathcal{T}^{(\mathcal{L})}$. The finest triangulation is also denoted by $\mathcal{T}_h = \mathcal{T}^{(0)}$. We denote by $h^{(\ell)}$ the typical size of $\mathcal{T}^{(\ell)}$. We assume that the spatial variation of $\kappa(x)$ is captured by the finest triangulation $\mathcal{T}_h = \mathcal{T}^{(0)}$, while the other meshes $\mathcal{T}^{(\ell)}$, $\ell = 1, \dots, \mathcal{L}$, may be too coarse to accurately resolve the spatial distribution of the coefficient.

We develop multilevel methods for the solution of elliptic finite element problems with multiscale high-contrast coefficients. We do not assume that the discontinuities of the coefficient are aligned with the coarse elements; hence, in each coarse block we can have *inclusions* and *channels* with no prescribed relative position with respect to the boundaries of the coarse blocks. In fact, our methods handle complex geometric distributions of the discontinuities. The two-level version of some of the methods studied here were proved in [5] to be robust with respect to the high-contrast of the media. The analysis and methods presented here are general and can be applied to general elliptic equations, see [9, 10] for an algebraic two-level setting. One example is flow problems, where the contrast in the coefficient is a very important physical parameter linked to the cost of obtaining a numerical solution of this equation.

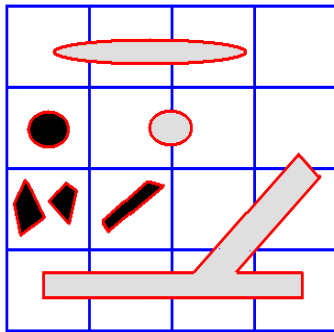


FIGURE 1. Schematic picture with channels (gray regions) and inclusions (black regions) with respect to coarse regions.

In order to simplify the presentation of our methods and to fix ideas, we make some assumptions on the meshes and the high-contrast coefficients. We assume that the fine mesh $\mathcal{T}_h = \mathcal{T}^{(0)}$ is sufficiently fine to accurately represent all variations of the coefficient κ . We assume that the coefficient κ has many high-contrast regions. The high-contrast regions are classified as high-contrast inclusions and channels. Inclusions and channels are defined with respect to a particular triangulation, in our setting $\mathcal{T}^{(j)}$, with $1 \leq j \leq \mathcal{L}$. For simplicity, a high-contrast region R is considered an isolated inclusion if there is a $\delta > 0$ ($\delta = O(h^{(j)})$) and an element $\tau \in \mathcal{T}^{(j)}$ such that $R \subset \tau$ and $\text{dist}(R, \partial\tau) > \delta$. If a high-contrast region is not an inclusion with respect to $\mathcal{T}^{(j)}$, then it is considered being a channel with respect to $\mathcal{T}^{(j)}$. See Figure 1 for an illustration. Note that a region can be classified as a channel with respect to a mesh $\mathcal{T}^{(\ell)}$ and also classified as an isolated inclusion with respect to another coarser grid. We assume that the coefficient κ is a simple function of high-contrast channels

and inclusions. More specifically, we assume that κ has form

$$(2.3) \quad \kappa = 1_B + \sum_{i=1}^{N_{ch}} \eta_i^C 1_{C_i} + \sum_{i=1}^{N_{in}} \eta_i^I 1_{I_i},$$

where $\eta_i^C \gg 1$, $i = 1, \dots, N_{ch}$ and $\eta_i^I \gg 1$, $i = 1, \dots, N_{in}$. Here, the regions $\{C_i\}_{i=1}^{N_{ch}}$ represent the high-conductivity channels and the regions $\{I_i\}_{i=1}^{N_{in}}$ represent the isolated inclusions. For a region R , we denote by 1_R its characteristic function; i.e., 1_R has value one in R and value zero elsewhere. The classification of channels and inclusions is made with respect to a fixed triangulation. Each high-contrast region (C_i or I_i) is connected and it is the union of fine grid elements; that is, $C_i = \cup_{\tau \subset C_i} \tau$, $i = 1, \dots, N_{ch}$ and $I_i = \cup_{\tau \subset I_i} \tau$, $i = 1, \dots, N_{in}$. The background region B has conductivity 1 and is generally a disconnected region. The contrast of κ in (2.3) is $\eta = \max\{\max \eta_i^C, \max \eta_i^I\}$. Finally, we assume that the geometry and topology of the inclusions and channels are independent of η .

Let $V^{(\ell)}$ be the finite element space of piecewise linear functions on $\mathcal{T}^{(\ell)}$, $\ell = 0, 1, \dots, \mathcal{L}$. The Galerkin formulation of (2.1) is to find $u^* \in V^{(0)} \cap H_0^1(D)$ with $a(u^*, v) = f(v)$ for all $v \in V^{(0)} \cap H_0^1(D)$. Or in matrix form

$$(2.4) \quad Au^* = b,$$

where for all $u, v \in V^{(0)}(D)$ we have $v^T Au = \int_D \kappa \nabla u \cdot \nabla v$, and $v^T b = \int_D f v$. We denote $A^{(0)} = A$. For each fine element $\tau \in \mathcal{T}^{(0)}$, let $A_\tau^{(0)}$ be the local finite element matrix. The fine-grid stiffness matrix $A^{(0)}$ can be obtained by the standard assembling procedure based on the local (element) matrices $A_\tau^{(0)}$, $\tau \in \mathcal{T}^{(0)}$.

3. AN ABSTRACT THREE-LEVEL METHOD

We present our method in a three-level setting. Therefore, in the present section, we assume $\mathcal{L} = 2$. The presentation in this section describes our recursion step in our multilevel formulation. In order to simplify the notation, we use $\mathcal{T}_h = \mathcal{T}^{(0)}$, $\tilde{\mathcal{T}}_{\tilde{H}} = \mathcal{T}^{(1)}$ and $\mathcal{T}_H = \mathcal{T}^{(2)}$. The superscript (0) is replaced by the script h . The superscript (1) will be replaced by the tilde notation and the superscript (2) will be omitted.

3.1. Intermediate coarse space assumptions. The space associated with the first-level triangulation, $\mathcal{T}_h = \mathcal{T}^{(0)}$, is $V^h = V^{(0)}$, the fine grid finite element space. In what follows, the space V^h can be replaced by any other (spectrally) constructed space as the one we design next. We denote by $V^h(\tilde{\omega})$ the restrictions of functions in V^h to a given subdomain $\tilde{\omega}$. We also denote by $V_0^h(\tilde{\omega})$ the space of functions in V^h that are supported in $\tilde{\omega}$.

Our main assumption is that we are given an abstract intermediate coarse space $\tilde{W}_{\tilde{H}} \subset V_0^h$ that admits basis functions $\{\tilde{w}_{j, \alpha}\}_{\{\alpha=0, \dots, \tilde{L}_j; \tilde{\mathbf{x}}_j \in \tilde{\mathcal{N}}_{\tilde{H}}\}}$ that are locally supported with respect to $\tilde{\mathcal{T}}_{\tilde{H}}$, i.e., each $\tilde{w}_{j, \alpha}$ is supported in the union of all elements from $\tilde{\mathcal{T}}_{\tilde{H}}$ that share the vertex $\tilde{\mathbf{x}}_j \in \tilde{\mathcal{N}}_{\tilde{H}}$. Note that we have assumed that each vertex $\tilde{\mathbf{x}}_j \in \tilde{\mathcal{N}}_{\tilde{H}}$ is associated with $\tilde{L}_j \geq 1$ basis functions supported in the neighborhood $\tilde{\omega}_j$ of all elements from $\tilde{\mathcal{T}}_{\tilde{H}}$ that share $\tilde{\mathbf{x}}_j$.

Let $\{\tilde{D}^{(j)} : V^h \rightarrow V^h\}$ be a partition of identity locally supported in $\tilde{\omega}_j$. That is,

$$(3.1) \quad \sum_{\tilde{\mathbf{x}}_j \in \tilde{\mathcal{N}}_{\tilde{H}}} \tilde{D}^{(j)} = Id_{V^h} \quad \text{and} \quad \text{Support}(\tilde{D}^{(j)}v) \subset \tilde{\omega}_j \text{ for all } v \in V^h.$$

Here, $Id_{V^h} : V^h \rightarrow V^h$ is the identity operator defined on V^h . Given a globally defined function $v \in V^h$, we use $\tilde{D}^{(j)}$ to define a locally supported function $\tilde{D}^{(j)}v$ that has support $\text{Support}(\tilde{D}^{(j)}v) \subset \tilde{\omega}_j$. In the analysis presented in this paper, applying the operator $\tilde{D}^{(j)}$ replaces the step of multiplication by partition of unity functions as used in [5, 6]. We make the following remark about the action of the partition of identity on locally defined functions.

Remark 3.1 (Notation). *Given a function $v \in V^h(\tilde{\omega}_j)$, we define the action of $\tilde{D}^{(s)}$ on v by*

$$\tilde{D}^{(s)}v = \tilde{D}^{(s)}E_0^{\tilde{\omega}_j}v,$$

where $E_0^{\tilde{\omega}_j}$ is the discrete extension by zero (to the degrees of freedom) outside ω_j . We note that $E_0^{\tilde{\omega}_j}w$ is the finite element function with zero value at the degrees of freedom outside $\tilde{\omega}_j$ so that $E_0^{\tilde{\omega}_j}w \in \tilde{V}^h$.

We also assume that $\tilde{W}_{\tilde{H}}$ admits an interpolant $\tilde{I}_{\tilde{H}} : V^h \rightarrow \tilde{W}_{\tilde{H}}$ such that the following local energy boundedness holds:

(A) For every $v \in V^h$ the interpolant $\tilde{I}_{\tilde{H}}v \in \tilde{W}_{\tilde{H}}$ satisfies the local approximation property for any $\tilde{\tau} \in \tilde{\mathcal{T}}_{\tilde{H}}$:

$$(3.2) \quad a_{\tilde{\tau}}(\tilde{D}^{(i)}(v - \tilde{I}_{\tilde{H}}v), \tilde{D}^{(i)}(v - \tilde{I}_{\tilde{H}}v)) \leq \tilde{\delta}_{\tilde{\tau}, \tilde{H}} \int_{\tilde{\omega}_{\tilde{\tau}}} \kappa |\nabla v|^2.$$

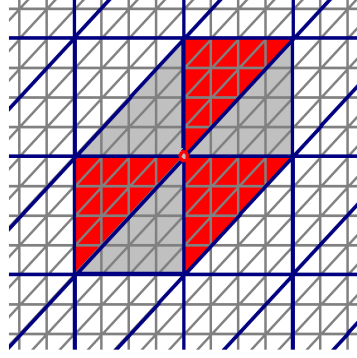
(B) The interpolant $\tilde{I}_{\tilde{H}}v \in \tilde{W}_{\tilde{H}}$ is bounded locally in energy, i.e., we have

$$(3.3) \quad a_{\tilde{\tau}}(\tilde{I}_{\tilde{H}}v, \tilde{I}_{\tilde{H}}v) = \int_{\tilde{\tau}} \kappa |\nabla \tilde{I}_{\tilde{H}}v|^2 \leq \tilde{\nu}_{\tilde{\tau}, \tilde{H}} a_{\tilde{\omega}_{\tilde{\tau}}}(v, v).$$

Here, $\tilde{\omega}_{\tilde{\tau}} = \cup_{\tilde{\mathbf{x}}_j \in \tilde{\tau}} \tilde{\omega}_j$.

Our goal is to construct and analyze a coarse space W_H and a coarse interpolation operator $I_H : \tilde{W}_{\tilde{H}} \rightarrow W_H$. Here, we present a general abstract construction that generalizes the methods presented in [11]. The resulting spaces will be nested (that is, $W_H \subset \tilde{W}_{\tilde{H}}$) as in the genuine multilevel method presented in [11]. The coarse space W_H is constructed using the coarse triangulation \mathcal{T}_H and the spectral AMGe method in the form proposed in [5, 11]. In the next section, we summarize the construction of local basis of W_H .

3.2. Construction of coarse basis functions. For each $\mathbf{x}_i \in \mathcal{N}_H$, we form the neighborhood set ω_i (similar to the previous level) as the union of elements from \mathcal{T}_H that share the coarse grid vertex \mathbf{x}_i . See Figure 2. Note that ω_i is also a union of elements from $\tilde{\mathcal{T}}_{\tilde{H}}$.

FIGURE 2. Coarse node x_i and coarse node neighborhood ω_i .

We denote by $\widetilde{W}_{\widetilde{H}}(\omega_i)$ the restrictions of functions in $\widetilde{W}_{\widetilde{H}}$ to the subdomain ω_i . We also denote by $\widetilde{W}_{\widetilde{H}}(\omega_i) \cap V_0^h(\omega_i)$ the space of functions in $\widetilde{W}_{\widetilde{H}}$ that are supported in $\widetilde{\omega}_i$. In particular, we identify functions in $\widetilde{W}_{\widetilde{H}}(\omega_i) \cap V_0^h(\omega_i)$ with their extension by zero outside ω_i .

For latter use, we define the maximum number of neighbors by

$$(3.4) \quad N_H = \max_i \{N_{\omega_i, H}\} = \max_{\tau \in \mathcal{T}_H} \{N_{\tau, H}\},$$

where

$$N_{\tau, H} = \#\{\tau' : \tau' \cap \tau \neq \emptyset\} \text{ and } N_{\omega_i, H} = \#\{s : \omega_s \cap \omega_i \neq \emptyset\}.$$

We assemble the local matrix \widetilde{A}_{ω_i} from the intermediate level matrices $\widetilde{A}_{\widetilde{\tau}}$ for all $\widetilde{\tau} \subset \omega_i$. The latter have entries $\int_{\widetilde{\tau}} k \nabla \widetilde{w}_{r, \alpha} \cdot \nabla \widetilde{w}_{s, \beta}$, where $\widetilde{\mathbf{x}}_r$ and $\widetilde{\mathbf{x}}_s$ are vertices from $\widetilde{\mathcal{T}}_{\widetilde{H}}$ and $\alpha \in \{0, \dots, \widetilde{L}_r\}$, $\beta \in \{0, \dots, \widetilde{L}_s\}$ correspond to the respective basis functions of $\widetilde{W}_{\widetilde{H}}$ restricted to $\widetilde{\tau}$. We assume that we have access to these element matrices (by assumption on the finest level, and achievable at all consecutive coarse levels by recursion).

We use a partition of identity based on the $\widetilde{W}_{\widetilde{H}}$ degrees of freedom. First, we assume that we have such a partition of identity and obtain abstract results. Later, in Section 4 we give examples of construction of suitable partitions of identity. Assume that we are given linear operators that form a locally supported partition of the identity $\{D^{(i)} : \widetilde{W}_{\widetilde{H}} \rightarrow \widetilde{W}_{\widetilde{H}}\}_{\mathbf{x}_i \in \mathcal{T}_H}$ such that

$$(3.5) \quad \sum_{\mathbf{x}_i \in \mathcal{N}_H} D^{(i)} = Id_{\widetilde{W}_{\widetilde{H}}} \quad \text{with} \quad \text{Support}(D^{(i)}w) \subset \omega_i \text{ for all } w \in \widetilde{W}_{\widetilde{H}}.$$

Here, $Id_{\widetilde{W}_{\widetilde{H}}}$ is the identity operator in $\widetilde{W}_{\widetilde{H}}$. We use the action of the partition of identity operators $D^{(i)}$ on functions defined on subdomains. See Remark 3.1. The partition of identity $\{D^{(i)}\}_{\mathbf{x}_i \in \mathcal{T}_H}$ is used to cut off global functions to local ones with zero trace on $\partial\omega_i$. This is a main ingredient to get a three-level stable decomposition.

Our main assumption on the partition of identity $\{D^{(i)}\}_{\mathbf{x}_i \in \mathcal{T}_H}$ is stated next. We assume that there is a local (positive definite) bilinear form \overline{m}_{ω_i} such that

$$(3.6) \quad \sum_{r,s} \int_{\omega_i} \kappa |\nabla D^{(r)} D^{(s)} w|^2 \leq C_{\overline{m}} \overline{m}_{\omega_i}(w, w) \quad \text{for all } w \in \widetilde{W}_{\widetilde{H}}.$$

In the next section, we give some examples of construction of partition of identity and bilinear forms \overline{m} . The choice of the partition of identity and the bilinear form \overline{m} are very important as they determine the dimension of the resulting (robust with respect to the contrast) coarse space W_H . We assemble the local matrix \widetilde{M}_{ω_i} which corresponds to the matrix representation of the bilinear form \overline{m}_{ω_i} in (3.6). These matrices \widetilde{M}_{ω_i} have entries $\overline{m}(w_{r,\alpha}, w_{s,\alpha})$. Then, we solve the local generalized eigenvalue problems of size \widetilde{N}_i (the number of degrees of freedom from $\widetilde{W}_{\widetilde{H}}$ associated with ω_i)

$$(3.7) \quad \widetilde{A}_{\omega_i} \mathbf{q}_m = \Lambda_m \widetilde{M}_{\omega_i} \mathbf{q}_m, \quad m = 1, \dots, \widetilde{N}_i,$$

which is the matrix form of the eigenvalue problem: find $\psi \in \widetilde{W}_{\widetilde{H}}(\omega_i) \cap V_0^h$ such that

$$(3.8) \quad a_{\omega_i}(\psi, w) = \Lambda_m \overline{m}_{\omega_i}(\psi, w), \quad \text{for all } w \in \widetilde{W}_{\widetilde{H}}(\omega_i) \cap V_0^h.$$

Note that the boundary condition for the eigenvalue problem above is a zero Dirichlet boundary condition in $\partial\omega_i \cap \partial D$ in case $\partial\omega_i \cap \partial D$ is not empty. For interior subdomains when $\partial\omega_i \cap \partial D$ is empty, a *natural* boundary condition on $\partial\omega_i$ is used. The eigenvalues $\Lambda_m = \Lambda_m^{(\omega_i)}$ are increasingly ordered. We split the spectrum in two parts by choosing an integer $L_i^H \leq \widetilde{N}_i$. All eigenvectors $\mathbf{q}_m = \mathbf{q}_m^{(\omega_i)}$ for $m \leq L_i^H$ are used to define the basis of the coarse space W_H . Since the eigenvectors of (3.8) do not vanish on $\partial\omega_i$, we use a cut-off procedure. To do this, we use the locally supported partition of identity $\{D^{(i)}\}$ of $\widetilde{W}_{\widetilde{H}}$ subordinated to the partition $\{\omega_i\}$ in (3.5).

Definition 3.1 (Definition of coarse basis).

We define the basis function of the coarse space W_H by

$$w_{i,\alpha}^H = D^{(i)} q_\alpha^{(\omega_i)}, \quad \alpha = 1, \dots, L_i^H.$$

Here, $q_\alpha^{(\omega_i)}$ stands for the finite element function that comes from the eigenvector $\mathbf{q}_\alpha^{(\omega_i)}$. See Remark 3 for a precise description of the action of the partition of identity operators on locally defined functions (vector of degrees of freedom). Note that $w_{i,\alpha}^H \in \widetilde{W}_{\widetilde{H}}$ and $\text{Support}(w_{i,\alpha}^H) \subset \omega_i$; that is, $w_{i,\alpha} \in \widetilde{W}_{\widetilde{H}}(\omega_i) \cap V_0^h(\omega_i)$.

Our next goal is to verify counterparts of assumptions (A)-(B) when $\widetilde{W}_{\widetilde{H}}$ is replaced with W_H . Given $w \in \widetilde{W}_{\widetilde{H}}$, define

$$(3.9) \quad I_H w = \sum_{\mathbf{x}_i \in \mathcal{N}_H} \sum_{\alpha=1}^{L_i^H} c_{i,\alpha} w_{i,\alpha}^H, \quad \text{where} \quad c_{i,\alpha} = (kw, q_\alpha^{(\omega_i)})_{\omega_i} := \int_{\omega_i} \kappa w q_\alpha^{(\omega_i)}.$$

Note that we can write

$$(3.10) \quad I_H w = \sum_{\mathbf{x}_i \in \mathcal{N}_H} D^{(i)} I_{L_i^H}^{\omega_i} w, \quad \text{where} \quad I_{L_i^H}^{\omega_i} w = \sum_{\alpha=1}^{L_i^H} c_{i,\alpha} q_\alpha^{(\omega_i)}.$$

From (3.6) and eigenvalue problem (3.7), we have,

$$(3.11) \quad \begin{aligned} \sum_{r,s} \int_{\omega_i} \kappa |\nabla D^{(r)} D^{(s)}(w - I_{L_i}^{\omega_i} w)|^2 &\leq C_{\bar{m}} \bar{m}_{\omega_i} (w - I_{L_i}^{\omega_i} w, w - I_{L_i}^{\omega_i} w) \\ &\leq C_{\bar{m}} \frac{1}{\Lambda_{L+1}} \int_{\omega_i} \kappa |\nabla w|^2. \end{aligned}$$

By using triangle inequality and Cauchy-Schwarz inequality, we obtain

$$(3.12) \quad \begin{aligned} \int_{\omega_i} \kappa |\nabla D^{(i)}(w - I_{L_i}^{\omega_i} w)|^2 &\leq \sum_r \int_{\omega_i} \kappa |\nabla D^{(r)}(\sum_s D^{(s)}(w - I_{L_i}^{\omega_i} w))|^2 \\ &\leq N_H \sum_{r,s} \int_{\omega_i} \kappa |\nabla D^{(r)} D^{(s)}(w - I_{L_i}^{\omega_i} w)|^2 \\ &\leq N_H C_{\bar{m}} \bar{m}_{\omega_i} (w - I_{L_i}^{\omega_i} w, w - I_{L_i}^{\omega_i} w) \\ &\leq N_H C_{\bar{m}} \frac{1}{\Lambda_{L_i^H+1}} \int_{\omega_i} \kappa |\nabla w|^2. \end{aligned}$$

Lemma 3.1. Consider I_H defined in (3.9). The following estimates hold:

(C) For every $w \in \widetilde{W}_{\widetilde{H}}$

$$(3.13) \quad a_\tau(D^{(i)}(w - I_H w), D^{(i)}(w - I_H w)) \leq \delta_{\tau,H} \int_{\omega_\tau} \kappa |\nabla w|^2,$$

where $\delta_{\tau,H} \leq N_H^2 C_{\bar{m}} \frac{1}{\Lambda_{L_i^H+1}}$.

(D) For every $w \in \widetilde{W}_{\widetilde{H}}$

$$(3.14) \quad a_\tau(I_H w, I_H w) = \int_\tau \kappa |\nabla I_H w|^2 \leq \nu_{\tau,H} a_{\omega_\tau}(w, w),$$

where $\nu_{\tau,H} \leq 2 + 2N_H^3 C_{\bar{m}} \max_{r \in \tau} \frac{1}{\Lambda_{L_i^H+1}}$.

Proof. From (3.10), using triangle inequality and Cauchy-Schwarz inequality, we obtain

$$(3.15) \quad \begin{aligned} &a_\tau(D^{(i)}(w - I_H w), D^{(i)}(w - I_H w)) \\ &= a_\tau\left(\sum_{x_r \in \tau} D^{(i)} D^{(r)}(w - I_{L_r^H}^{\omega_r} w), \sum_{x_r \in \tau} D^{(i)} D^{(r)}(w - I_{L_r^H}^{\omega_r} w)\right) \\ &\leq N_H \sum_{x_r \in \tau} a_\tau(D^{(i)} D^{(r)}(w - I_{L_r^H}^{\omega_r} w), D^{(i)} D^{(r)}(w - I_{L_r^H}^{\omega_r} w)) \\ &\leq N_H \sum_{x_r \in \tau} a_{\omega_r}(D^{(i)} D^{(r)}(w - I_{L_r^H}^{\omega_r} w), D^{(i)} D^{(r)}(w - I_{L_r^H}^{\omega_r} w)) \\ &\leq N_H \sum_{x_r \in \tau} C_{\bar{m}} m_{\omega_r} (w - I_{L_i^H}^{\omega_i} w, w - I_{L_i^H}^{\omega_i} w) \leq N_H^2 C_{\bar{m}} \frac{1}{\Lambda_{L_i^H+1}} \int_{\omega_\tau} \kappa |\nabla w|^2. \end{aligned}$$

To prove equation (3.14), we proceed in a similar way. We have

$$(3.16) \quad a_\tau(I_H w, I_H w) \leq 2a_\tau(w - I_H w, w - I_H w) + 2a_\tau(w, w).$$

Using (3.12) to bound the first term above, we have

$$\begin{aligned}
a_\tau(w - I_H w, w - I_H w) &= a_\tau\left(\sum_{x_r \in \tau} D^{(r)}(w - I_{L_r^H}^{\omega_r} w), \sum_{x_r \in \tau} D^{(r)}(w - I_{L_r^H}^{\omega_r} w)\right) \\
&\leq N_H \sum_{x_r \in \tau} a_\tau(D^{(r)}(w - I_{L_r^H}^{\omega_r} w), D^{(r)}(w - I_{L_r^H}^{\omega_r} w)) \\
&\leq N_H \sum_{x_r \in \tau} a_{\omega_r}(D^{(r)}(w - I_{L_r^H}^{\omega_r} w), D^{(r)}(w - I_{L_r^H}^{\omega_r} w)) \\
&\leq N_H \sum_{x_r \in \tau} N_H C_{\bar{m}} \frac{1}{\Lambda_{L+1}} \int_{\omega_r} \kappa |\nabla w|^2 \\
(3.17) \quad &\leq N_H^2 C_{\bar{m}} \frac{1}{\Lambda_{L+1}} \sum_{x_r \in \tau} \int_{\omega_r} \kappa |\nabla w|^2 \leq N_H^3 C_{\bar{m}} \frac{1}{\Lambda_{L+1}} \int_{\omega_\tau} \kappa |\nabla w|^2.
\end{aligned}$$

We then have

$$a_\tau(I_H w, I_H w) \leq (2 + 2N_{\tau, H}^3 C_{\bar{m}}) a_{\omega_\tau}(w, w).$$

□

3.3. A two-level stable decomposition. In this section, we obtain stable decomposition for functions in $\widetilde{W}_{\widetilde{H}}$ using the coarse space W_H and the local spaces $\{\widetilde{W}_{\widetilde{H}} \cap V_0^h(\omega_i)\}_{x_i \in \mathcal{T}_H}$. Note that the local space $\widetilde{W}_{\widetilde{H}} \cap V_0^h(\omega_i)$ consists of functions in $\widetilde{W}_{\widetilde{H}}$ that are supported in the subdomain ω_i .

Theorem 3.1. *For every $w \in \widetilde{W}_{\widetilde{H}}$ there exists a decomposition of w , and a positive constant \widetilde{C}_0^2 , such that*

$$w = w_2 + \sum_{x_i \in \mathcal{T}_H} w_{1,i},$$

with $w_2 \in W_H$, $w_{1,i} \in \widetilde{W}_{\widetilde{H}} \cap V^h(\omega_i)$ and

$$(3.18) \quad a(w_2, w_2) + \sum_{x_i \in \mathcal{T}_H} a_{\omega_i}(w_{1,i}, w_{1,i}) \leq \widetilde{C}_0^2 a(w, w),$$

with $\widetilde{C}_0^2 \leq N_H(\nu_H + \delta_H)$. Here, $\nu_H = \max_{\tau \in \mathcal{T}_H} \{\nu_{\tau, H}\}$, $\delta_H = \max_{i \in \mathcal{N}_H} \{\delta_{\omega_i, H}\}$ and $N_H = \max_{\tau \in \mathcal{T}_H} \{N_\tau\}$.

Proof. Recall that $\{D^{(i)} : \widetilde{W}_{\widetilde{H}} \rightarrow \widetilde{W}_{\widetilde{H}}\}_{x_i \in \mathcal{N}_H}$ is a partition of identity subordinated to $\{\omega_i\}_{x_i \in \mathcal{N}_H}$. Given $w \in \widetilde{W}_{\widetilde{H}}$, we define

$$w_2 = I_H w \in W_H, \quad w_1 = w - I_H w \in \widetilde{W}_{\widetilde{H}}$$

and

$$w_{1,i} = D^{(i)} w_1 \in \widetilde{W}_{\widetilde{H}} \cap V_0^h(\omega_i).$$

We use the notation $N_{\tau, H} = \#\{\tau' \in \mathcal{T}_H : \tau' \cap \tau \neq \emptyset\}$. We bound the first term in (3.18). Using property (D) in (3.14), we have

$$a(w_2, w_2) = \sum_{\tau} \int_{\tau} \kappa |\nabla I_H w|^2 \leq \sum_{\tau} \nu_{\tau, H} a_{\omega_\tau}(w, w) \leq \nu_H N_H \int_D \kappa |\nabla w|^2.$$

Then, we can bound

$$(3.19) \quad a(w_2, w_2) \leq \nu_H N_H a(w, w).$$

Now we estimate the second term in (3.18). We use (3.13) to get

$$(3.20) \quad a_{\omega_i}(w_{1,i}, w_{1,i}) = \int_{\omega_i} \kappa |\nabla(D^{(i)}(w - I_H w))|^2 \leq \delta_{\omega_i, H} \int_{\omega_i} \kappa |\nabla w|^2$$

and we can write

$$(3.21) \quad \sum_{x_i \in \mathcal{T}_H} a_{\omega_i}(w_{1,i}, w_{1,i}) \leq \sum_{x_i \in \mathcal{T}_H} \delta_{\omega_i, H} \int_{\omega_i} \kappa |\nabla w|^2 \leq N_H \delta_H \int_D |\nabla w|^2.$$

Finally, we bound the energy of the decomposition using (3.19) and (3.21). We get,

$$a(w_2, w_2) + \sum_{x_i \in \mathcal{T}_H} a_{\omega_i}(w_{1,i}, w_{1,i}) \leq (\nu_H N_H + N_H \delta_H) a(w, w) \leq \tilde{C}_0^2 a(w, w).$$

This finishes the proof. \square

3.4. A three level stable decomposition. Now, we obtain a stable decomposition considering the subspaces

$$\{W_H\} \cup \{\widetilde{W}_{\tilde{H}} \cap V_0^h(\omega_i)\}_{x_i \in \mathcal{T}_H} \cup \{V_0^h(\tilde{\omega}_j)\}_{\tilde{x}_j \in \tilde{\mathcal{T}}_{\tilde{H}}}.$$

Note that $W_H \subset \widetilde{W}_{\tilde{H}} \subset V^h(D)$. Note also that W_H corresponds to the coarse space related to the triangulation $\mathcal{T}_H = \mathcal{T}^{(2)}$. The space $\widetilde{W}_{\tilde{H}}$ corresponds to the coarse space of triangulation $\tilde{\mathcal{T}}_{\tilde{H}} = \mathcal{T}^{(1)}$. Then, $\widetilde{W}_{\tilde{H}} \cap V_0^h(\omega_i)$ corresponds to a local subdomain subspace at the level (1). The subspace $V_0^h(\tilde{\omega}_j) = V^h \cap V_0^h(\tilde{\omega}_j)$ corresponds to a local space at the finest level, at the level (0).

Theorem 3.2. *For every $v \in V$ there exist a decomposition of v and a positive constant C_0 such that*

$$v = v_2 + \sum_{\mathbf{x}_i \in \mathcal{N}_H} v_{1,i} + \sum_{\tilde{\mathbf{x}}_j \in \tilde{\mathcal{N}}_{\tilde{H}}} v_{0,j},$$

with $v_2 \in W_H$, $v_{1,i} \in \widetilde{W}_{\tilde{H}} \cap V_0^h(\omega_i)$, $\mathbf{x}_i \in \mathcal{N}_H$; $v_{0,j} \in V_0^h(\tilde{\omega}_j)$, $\tilde{\mathbf{x}}_j \in \tilde{\mathcal{N}}_{\tilde{H}}$; and

$$(3.22) \quad a(v_2, v_2) + \sum_{\mathbf{x}_i \in \mathcal{N}_H} a_{\omega_i}(v_{1,i}, v_{1,i}) + \sum_{\tilde{\mathbf{x}}_j \in \tilde{\mathcal{N}}_{\tilde{H}}} a_{\tilde{\omega}_j}(v_{0,j}, v_{0,j}) \leq C_0^2 a(v, v)$$

where $C_0^2 \leq \tilde{N}_{\tilde{H}}(\tilde{C}_0^2 \tilde{\nu}_{\tilde{H}} + \tilde{\delta}_{\tilde{H}}) < \tilde{N}_{\tilde{H}} N_H (\nu_H + \delta_H) (\tilde{\nu}_{\tilde{H}} + \tilde{\delta}_{\tilde{H}})$.

Proof. Recall that $\{D^{(i)} : \widetilde{W}_{\tilde{H}} \rightarrow \widetilde{W}_{\tilde{H}}\}_{\mathbf{x}_i \in \mathcal{N}_H}$ and $\{\tilde{D}^{(j)} : V_h \rightarrow V_h\}_{\tilde{\mathbf{x}}_j \in \tilde{\mathcal{N}}_{\tilde{H}}}$ are partitions of identity subordinated to $\{\omega_i\}_{\mathbf{x}_i \in \mathcal{N}_H}$ and $\{\tilde{\omega}_j\}_{\tilde{\mathbf{x}}_j \in \tilde{\mathcal{N}}_{\tilde{H}}}$, respectively. Given $v \in V_h$, we define

$$v_2 = I_H(\tilde{I}_{\tilde{H}} v) \in W_H, \quad v_1 = \tilde{I}_{\tilde{H}} v - I_H(\tilde{I}_{\tilde{H}} v) \in \widetilde{W}_{\tilde{H}}, \quad v_0 = v - \tilde{I}_{\tilde{H}} v \in V_h$$

and

$$v_{1,i} = D^{(i)} v_1 \in \widetilde{W}_{\tilde{H}} \cap V_0^h(\omega_i) \quad v_{0,j} = \tilde{D}^{(j)} v_0 \in V_0^h(\tilde{\omega}_j).$$

From Lemma 3.1 with $w = \tilde{I}_{\tilde{H}}v$, we have that

$$a(v_2, v_2) + \sum_{\mathbf{x}_i \in \mathcal{N}_H} a_{\omega_i}(v_{1,i}, v_{1,i}) \leq \tilde{C}_0^2 a(\tilde{I}_{\tilde{H}}v, \tilde{I}_{\tilde{H}}v).$$

We use property (B) in (3.3) and get

$$(3.23) \quad \int_D \kappa |\tilde{\nabla} \tilde{I}_{\tilde{H}}v|^2 = \sum_{\tilde{\tau}} \int_{\tilde{\tau}} |\kappa \nabla \tilde{I}_{\tilde{H}}v|^2 \leq \sum_{\tilde{\tau}} \nu_{\tilde{\tau}, \tilde{H}} a_{\omega_{\tilde{\tau}}}(v, v) \leq \tilde{\nu}_{\tilde{\tau}, \tilde{H}} \tilde{N}_{\tilde{H}} \int_D \kappa |\nabla v|^2.$$

Then, we can bound

$$(3.24) \quad a(v_2, v_2) + \sum_{\mathbf{x}_i \in \mathcal{T}_H} a_{\omega_i}(v_{1,i}, v_{1,i}) \leq \tilde{C}_0^2 \tilde{\nu}_{\tilde{H}} \tilde{N}_{\tilde{H}} a(v, v).$$

Now, we estimate the third term on the right-hand-side of (3.22). From (3.2), we get

$$(3.25) \quad a_{\tilde{\tau}}(v_{0,j}, v_{0,j}) = \int_{\tilde{\tau}} \kappa |\nabla(\tilde{D}^{(j)}(v - \tilde{I}_{\tilde{H}}v))|^2 \leq \tilde{\delta}_{\tilde{\tau}, \tilde{H}} \int_{\tilde{\omega}_{\tilde{\tau}}} \kappa |\nabla v|^2.$$

Then, using (3.25) we can write

$$(3.26) \quad \sum_{\tilde{\mathbf{x}}_j \in \tilde{\mathcal{N}}_{\tilde{H}}} a_{\tilde{\omega}_j}(v_{0,j}, v_{0,j}) \leq \sum_{\tilde{\mathbf{x}}_j \in \tilde{\mathcal{N}}_{\tilde{H}}} \tilde{\delta}_{\tilde{\omega}_j, \tilde{H}} \int_{\tilde{\omega}_j} \kappa |\nabla v|^2 \leq \tilde{N}_{\tilde{H}} \tilde{\delta}_{\tilde{H}} \int_D |\nabla v|^2.$$

Finally, we bound the energy of the decomposition using (3.26) and (3.24). We get,

$$\begin{aligned} a(v_2, v_2) + \sum_{\mathbf{x}_i \in \mathcal{N}_H} a_{\omega_i}(v_{1,i}, v_{1,i}) + \sum_{\tilde{\mathbf{x}}_j \in \tilde{\mathcal{N}}_{\tilde{H}}} a_{\omega_i}(v_{0,j}, v_{0,j}) &\leq (\tilde{C}_0^2 \tilde{\nu}_{\tilde{H}} \tilde{N}_{\tilde{H}} + \tilde{N}_{\tilde{H}} \tilde{\delta}_{\tilde{H}}) a(v, v) \\ &\leq \tilde{N}_{\tilde{H}} (\tilde{C}_0^2 \tilde{\nu}_{\tilde{H}} + \tilde{\delta}_{\tilde{H}}) a(v, v). \end{aligned}$$

This finishes the proof. \square

4. EXAMPLES OF PARTITIONS OF IDENTITY

In this section, we give examples of choices of partition of identity operators and eigenvalue problems. We consider two- and three-level version of the abstract method presented before.

4.1. The two-level version. We consider the two-level version; see [5]. We recall that the construction summarized in the last section was used in [5] to construct the coarse space $\tilde{W}_{\tilde{H}}$ starting with the fine grid \mathcal{T}_h and only one coarse grid $\tilde{\mathcal{T}}_{\tilde{H}}$. There, it is introduced the two level version of the method extended here to a multilevel version. We first give an example of a coarse space and the partition of identity satisfying assumption (3.1). In [5], the partition of identity operators are defined as

$$(4.1) \quad \tilde{D}^{(j)}v = I^h(\tilde{\chi}_j v),$$

where $\{\tilde{\chi}_j\}$ is a partition of unity subordinated to the decomposition $\{\tilde{\omega}_i\}$ with $|\nabla \tilde{\chi}_i|^2 \leq C_{pu} \frac{1}{H^2}$. Here, I^h denotes the fine-scale interpolation. Note that the matrix

form of $\tilde{D}^{(j)}$ is diagonal. To obtain properties (A) and (B), we introduce the bilinear form $\bar{m}_{\tilde{\omega}_j}$ such that

$$(4.2) \quad \sum_{r,s} \int_{\tilde{\omega}_i} \kappa |\nabla \tilde{D}^{(r)} \tilde{D}^{(s)} v|^2 \leq C_{\bar{m}} \bar{m}_{\tilde{\omega}_i}(v, v) \quad \text{for all } v \in V_h.$$

In [5], the bilinear form $\bar{m}_{\tilde{\omega}_i}$ is chosen to be defined by

$$\bar{m}_{\tilde{\omega}_i}(v, v) = \int_{\tilde{\omega}_i} \kappa |\nabla v|^2 + \frac{1}{H^2} \int_{\tilde{\omega}_i} \kappa v^2 \quad \text{for all } v \in V^h(\tilde{\omega}_i).$$

Using the analysis in [5], we can verify (4.2). Properties (A) and (B) can also be verified. The corresponding eigenvalue problem (for interior subdomains) is to find $\psi \in V^h(\tilde{\omega}_j)$ such that

$$(4.3) \quad a_{\tilde{\omega}_j}(\psi, v) = \Lambda_\ell \bar{m}_{\tilde{\omega}_j}(\psi, v), \quad \text{for all } v \in V^h(\tilde{\omega}_j).$$

The eigenvalues above are of the form

$$\Lambda_\ell = \frac{1}{1 + \frac{1}{\tilde{H}^2 \lambda_\ell}} \quad \text{or} \quad \frac{1}{\Lambda_\ell} = 1 + \frac{1}{\tilde{H}^2 \lambda_\ell},$$

where λ_ℓ are the eigenvalues of the problem,

$$\int_{\tilde{\omega}_j} \kappa \nabla \psi \cdot \nabla w = \lambda_\ell \int_{\tilde{\omega}_j} \kappa \psi w \quad \text{for all } v \in V^h(\tilde{\omega}_j).$$

A main observation is that only a few eigenvalues $\{\lambda_\ell\}$ vanish asymptotically as the contrast increases. The number of small eigenvalues is related to the number of high-contrast regions (channel and inclusions with respect to $\tilde{\mathcal{T}}_{\tilde{H}}$). See [5, 6, 8] for more details.

In [7, 6], a partition of unity $\{\chi_j\}$, subordinated to the covering $\{\tilde{\omega}_j\}$, was introduced and a different eigenvalue problem was used. The bilinear form $\bar{m}_{\tilde{\omega}_j}$ and the partition of identity are given by

$$\bar{m}_{\tilde{\omega}_j}(v, v) = \int_{\tilde{\omega}_j} \kappa |\nabla v|^2 + \frac{1}{\tilde{H}^2} \int_{\tilde{\omega}_j} (\tilde{H}^2 \sum_r \kappa |\nabla \chi_r|^2) v^2 \quad \text{and} \quad D^{(j)} v = I^h(\chi_j v).$$

As before, only a few eigenvalues vanish asymptotically as the contrast increases. The number of small eigenvalues corresponds to the number of regions where the pointwise energy $\bar{\kappa} = \tilde{H}^2 \sum_r \kappa |\nabla \chi_r|^2$ has high value. For the latter, the eigenvalues are related to the eigenvalue problem

$$\int_{\tilde{\omega}_j} \kappa \nabla \psi \cdot \nabla v = \lambda_\ell \int_{\tilde{\omega}_j} \bar{\kappa} \psi v \quad \text{for all } v \in V_h(\tilde{\omega}_j).$$

For instance, if $\{\chi_j\}$ is the usual $P^1(\tilde{\mathcal{T}}_{\tilde{H}})$ piecewise linear partition of unity functions, then, the number of small eigenvalues is the number of high-contrast regions with the original coefficient κ . This is due to the fact that the gradient of the piecewise linear partition of unity is piecewise constant (of order $1/\tilde{H}^2$) in each block $\tilde{\tau} \in \tilde{\mathcal{T}}_{\tilde{H}}$. A better choice of a partition of unity is the case where $\{\chi_j\}$ are multi-scale functions with linear boundary condition. In this case, the pointwise energy κ becomes an order $O(1)$ number inside high-contrast inclusions with respect to $\tilde{\mathcal{T}}_{\tilde{H}}$

and it is of order $O(\eta)$ in the high-contrast long channels with respect to $\widetilde{\mathcal{T}}_{\widetilde{H}}$, where long channels are defined as high-conductivity inclusions connecting two edges of the coarse region. The resulting coarse spaces $\widetilde{W}_{\widetilde{H}}$ will have a smaller dimension and include relevant information that cannot be localized within coarse blocks $\widetilde{\tau}$. More sophisticated choices of partition of unity and partition of identity operators can also be considered that reduce even more the dimension of the coarse space; see [7, 6].

In this paper, we consider

$$(4.4) \quad \overline{m}_{\widetilde{\omega}_i}(v, v) := \sum_{r,s} \int_{\widetilde{\omega}_i} \kappa |\nabla \widetilde{D}^{(r)} \widetilde{D}^{(s)} v|^2 \quad \text{for all } v \in V_h(\omega_i).$$

Observations similar to the remarks above are also true for the number of eigenvalues if we use the bilinear for $\overline{m}_{\widetilde{\omega}_i}$ in (4.4). See Lemma 4.1 below where we prove that, under adequate assumptions on the partition of identity, the number of high-contrast asymptotically small eigenvalues corresponds to the number of channels. Under weaker assumptions on the partition of identity, the number of small eigenvalues corresponds to the number of inclusions and channels.

4.2. The three-level version. In this section we give examples of partition of identity operators $\{D^{(i)}\}$ and weighting bilinear form \overline{m} satisfying (3.6). As in the previous section, the partition of identity operators have diagonal matrix representation. We assume $\mathcal{L} = 2$, and, as before, we use the notation $\mathcal{T}_h = \mathcal{T}^{(0)}$, $\widetilde{\mathcal{T}}_{\widetilde{H}} = \mathcal{T}^{(1)}$ and $\mathcal{T}_H = \mathcal{T}^{(2)}$. We consider partition of unity functions $\{\chi_i\}$ such that

$$\sum_i \chi_i = 1, \text{ and } \chi_i \in P^1(\widetilde{\mathcal{T}}_{\widetilde{H}}) \text{ with } \text{Support}(\chi_i) \subset \omega_i.$$

Recall that $\{w_{s,\alpha}\}_{\widetilde{\mathbf{x}}_s \in \widetilde{\mathcal{N}}_{\widetilde{H}}}$ denote the finite element basis functions of $\widetilde{W}_{\widetilde{H}}$. We assume $P^1(\widetilde{\mathcal{T}}_{\widetilde{H}}) \subset \widetilde{W}_{\widetilde{H}}$. We have, in general, $P^1(\widetilde{\mathcal{T}}_{\widetilde{H}}) \neq \widetilde{W}_{\widetilde{H}}$ since we may have several degrees of freedom associated to each node $\widetilde{\mathbf{x}}_i$. We can write

$$\chi_i = \sum_{s,\alpha} \chi_{s,\alpha}^{(i)} w_{s,\alpha}.$$

For any $w \in \widetilde{W}_{\widetilde{H}}$ with $w = \sum_{s,\alpha} c_{s,\alpha} w_{s,\alpha}$, define

$$(4.5) \quad D^{(i)} w = \sum_{s,\alpha} \chi_{s,\alpha}^{(i)} c_{s,\alpha} w_{s,\alpha}.$$

Note that the matrix representation of $D^{(i)}$ with respect to the basis $\{w_{s,\alpha}\}_{\widetilde{\mathbf{x}}_s \in \mathcal{T}_H}$ is diagonal where the entries on the diagonal of $D^{(i)}$ correspond to the degrees of freedom of the function χ_i . Note also that if we denote

$$(4.6) \quad \Phi^{(i)} = \sum_{\widetilde{\mathbf{x}}_s \in \omega_i} \sum_{\alpha=1}^{\widetilde{L}_s} w_{s,\alpha},$$

we have

$$D^{(i)} \Phi^{(i)} = \chi_i.$$

The next lemma, Lemma 4.1, tells us the kind of functions $\{\chi_i\}$ we need to construct so we can get: 1) robustness with respect to the high-contrast and 2) minimal dimension coarse spaces. First, we need to introduce some notation.

As mentioned in (4.4), we consider

$$(4.7) \quad \bar{m}_{\omega_i}(w, w) := \sum_{r,s} \int_{\omega_i} \kappa |\nabla D^{(r)} D^{(s)} w|^2 \text{ for all } w \in \widetilde{W}_{\widetilde{H}}(\omega_i).$$

For a subregion $R \subset D$, we define the number P_R by

$$(4.8) \quad P_R = \sup_{w \in W_{\widetilde{H}}, \int_R w = 0} \frac{\sum_{r,s} \int_R |\nabla D^{(r)} D^{(s)} w|^2}{\int_R |\nabla w|^2}.$$

If $w \in \widetilde{W}_{\widetilde{H}}$ with $\int_R w = 0$ implies $w = 0$ on R , we define $P_R = 0$.

Remark 4.1. Assume that the numerator in (4.8) is replaced by the form

$$\int_R |\nabla w|^2 + \frac{1}{H^2} \int_R w^2$$

as in [11, 5, 6]. In this case, the standard Poincaré inequality gives that P_R is an order $O(1)$ number (independent of η).

Remark 4.2. For a general partition of identity $\{D^{(i)}\}$, we can write

$$(4.9) \quad \int_R \kappa |\nabla D^{(r)} D^{(s)} w|^2 \leq P_R^2 \int_R \kappa |\nabla w|^2, \text{ for all } w \in \widetilde{W}_{\widetilde{H}} \text{ with } \int_R w = 0.$$

We note that P_R depends only on the region R and the partition of identity $\{D^{(i)}\}$. The numbers P_R measure the variation introduced by the partition of the identity in the region R . In particular, if the partition of identity is such that for every subdomain ω_i , there is a constant $0 < d_R^{(i)} \leq 1$ with $D^{(i)} w = d_R^{(i)} w$ in the region R , then we see that P_R is an order one number $P_R \leq \max_{\omega_r \cap R \neq \emptyset} (d_R^{(r)})^2$. In the analysis below, the constant P_R will replace a Poincaré inequality constant used in [6, 5] for the analysis of the corresponding two-level method.

In the next result, we verify that the number of small (contrast dependent) eigenvalues is related to the number of high-contrast regions. We show that if the partition of identity is properly selected, then, the number of small eigenvalues is related only to the number of channels. The key idea is to assume that the action of the partition of identity does not introduce any variation to functions inside high-contrast inclusions. This is stated precisely in Assumption (2) in Lemma 4.1. In Section 4, we present some examples of partitions of identity that satisfy Assumption (2) in Lemma 4.1. The main purpose of Assumption (2) in Lemma 4.1 is to avoid small eigenvalues due to inclusions and to ensure that only small eigenvalues due to channels appear. If Assumption (2) in Lemma 4.1 does not hold, then, in general, the number of small (contrast dependent) eigenvalues, will be given by the number of inclusions and channels; see Remark 4.3.

Lemma 4.1. *Let the coefficient κ be of the form*

$$(4.10) \quad \kappa = 1_B + \sum_{i=1}^{N_{ch}} \eta_i^C 1_{C_i} + \sum_{i=1}^{N_{in}} \eta_i^I 1_{I_i},$$

where $\{C_i\}_{i=1}^{N_{ch}}$ represent the high-conductivity channels and $\{I_i\}_{i=1}^{N_{in}}$ represent the isolated inclusions. Assume that:

- (1) For every channel C_i , the number P_{C_i} defined in (4.8) does not depend on η_i^C .
- (2) The partition of identity $\{D^{(i)}\}$ satisfies: for every inclusion I_i there are constants $0 < R_{I_i} \leq 1$ independent of the contrast, such that

$$(4.11) \quad \int_{I_i} \kappa |\nabla D^{(r)} D^{(s)} w|^2 \leq R_{I_i} \int_{I_i} \kappa |\nabla w|^2, \quad \text{for all } w \in \widetilde{W}_{\widetilde{H}}.$$

Then, the eigenvalue problem,

$$(4.12) \quad a_{\omega_i}(\psi, w) = \Lambda_m \overline{m}_{\omega_i}(\psi, w), \quad \text{for all } w \in \widetilde{W}_{\widetilde{H}}(\omega_i),$$

has at most $N_{ch} + 1$ asymptotically vanishing eigenvalues when $\eta_i^C \rightarrow \infty$, $\eta_i^I \rightarrow \infty$.

Proof. We prove that there are at most $N = N_{ch}$ small eigenvalues. We have that

$$\lambda_{N+1} = \min_{\dim(V)=N+1} \max_{v \in V \setminus \{0\}} R(v),$$

where

$$R(v) = \frac{v^T \widetilde{A}^{(\omega_i)} v}{v^T \widetilde{M} v},$$

where $\widetilde{A}^{(\omega_i)}$ and \widetilde{M} are matrix forms of the bilinear forms introduced in Section 3.2. Then we have to show that for every $N + 1$ dimensional subspace $V (\subset \widetilde{W}_{\widetilde{H}}(\omega_i))$ there exists a vector $v \in V$ such that $R(v) \geq 1$.

Define the subspace

$$W_{\text{poin}} = \{w \in \widetilde{W}_{\widetilde{H}}(\omega_i) : \int_{\omega_i} w = 0 \text{ and } \int_{C_m} w = 0, m = 1, \dots, N = N_{ch}\}.$$

The subspace W_{poin} is of co-dimension $N + 1 = N_{ch} + 1$. From (4.8) with $R = C_m$, we can write

$$\sum_{r,s} \int_{C_m} |\nabla D^{(r)} D^{(s)} w|^2 \leq P_{C_m} \int_{C_m} |\nabla w|^2, \quad \text{for all } w \in W_{\text{poin}},$$

where P_{C_m} is independent of η ; or, multiplying by $\eta_m^C - 1 > 0$,

$$\sum_{r,s} (\eta_m^C - 1) \int_{C_m} |\nabla D^{(r)} D^{(s)} w|^2 \leq P_{C_m} (\eta_m^C - 1) \int_{C_m} |\nabla w|^2, \quad \text{for all } w \in W_{\text{poin}}.$$

We can use (4.8) with $R = \omega_i$ to have

$$\sum_{r,s} \int_{\omega_i} |\nabla D^{(r)} D^{(s)} w|^2 \leq P_{\omega_i} \int_{\omega_i} |\nabla w|^2, \quad \text{for all } w \in W_{\text{poin}},$$

where P_{ω_i} is independent of η . Adding these last two inequalities and (4.11), we then obtain

$$\sum_{r,s} \int_{\omega_i} \kappa |\nabla D^{(r)} D^{(s)} w|^2 \leq \max\{\max_{C_i} P_{C_i}, \max_{I_i} R_{I_i}, P_{\omega_i}\} \int_{\Omega} \kappa |\nabla w|^2, \text{ for all } w \in W_{\text{poin}}.$$

Let $V \subset \widetilde{W}_{\widetilde{H}}(\omega_i)$ be a subspace of dimension $N + 2$. We have that V and W_{poin} intersect in a subspace of dimension at least one. Then, we can select $w \in V \cap W_{\text{poin}}$ with $w \neq 0$; for this vector we have that

$$R(w) = \frac{w^T \widetilde{A}^{(\omega_i)} w}{w^T \widetilde{M} w} = \frac{\int_{\omega_i} \kappa |\nabla w|^2}{\sum_{r,s} \int_{\omega_i} \kappa |\nabla D^{(r)} D^{(s)} w|^2} \geq \frac{1}{\max\{\max_{C_i} P_{C_i}, \max_{I_i} R_{I_i}, P_{\omega_i}\}}.$$

□

Remark 4.3. *An analogous result is obtained if (2) is replaced by (2') as defined below.*

(2') *For every inclusion I_i , the number P_{I_i} defined in (4.8) does not depend on η_i . In this case, the number of small eigenvectors is related to the number of high-contrast regions, channels and inclusions. We define $W_{\text{poin}} = \{w \in \widetilde{W}_{\widetilde{H}}(\omega_i) : \int_{\omega_i} w = 0, \int_{C_m} w = 0, m = 1, \dots, N_{ch}, \text{ and } \int_{I_m} w = 0, m = 1, \dots, N_{in}\}$.*

Remark 4.4. *In order to work with Assumption (2) instead of (2'), the idea is then to construct the partition of identity $\{D^{(i)}\}$ where the degrees of freedom associated with inclusions have small or no variation. For instance, a useful partition of identity would have constant value in all degrees of freedom associated to a single inclusion.*

4.2.1. *Example of partition of identity using piecewise linear partition of unity.* Assume that the first level partition of identity is defined by using the piecewise (bi)linear partition of unity $\{\tilde{\chi}_j \in P^1(\widetilde{\mathcal{T}}_{\widetilde{H}})\}$. Introduce the linear partition of unity function $\{\chi_i^{lin} \in P^1(\mathcal{T}_H)\}$. In this case, we can write

$$\chi_i^{lin} = \sum_s e_s^{(i)} \tilde{z}_{\tilde{x}_s},$$

where $\tilde{z}_{\tilde{x}_s} \in P^1(\mathcal{T}_H)$ is a usual nodal basis function. We use the functions $\{\chi_i \in \widetilde{W}_{\widetilde{H}}\}$ defined by

$$\chi_i = \sum_r \sum_{\alpha=1}^{L_r} \chi_{r,\alpha}^{(i)} w_{r,\alpha} \quad \text{where} \quad \chi_{r,\alpha}^{(i)} = e_r^{(i)}, \text{ for } \alpha = 1, \dots, L,$$

and define $\{D^{(i)}\}$ as in (4.5). According to Remark 4.2, we can expect this coarse space to include basis functions for each inclusion and channel with respect to $\widetilde{\mathcal{T}}_{\widetilde{H}}$ (or \mathcal{T}_H).

As an illustrative example, let us consider the coefficient and meshes depicted in Figure 3. Gray regions indicate the high-contrast regions. The coefficient κ has the value 10^4 inside high-contrast regions and value 1 on the background region.

The small relevant eigenvalue information is illustrated in Figure 4.

- (1) At the first level, all the subdomains have only one zero eigenvalue. No small eigenvalue is present.
- (2) At the second level, there are subdomains with two and three small eigenvalues. This is expected since, at this level, some coarse node neighborhoods may include up to three of the high-contrast regions. See Figure 3.
- (3) At the third level, there are subdomains with two, three and four small eigenvalues. This is expected due to the number of high-contrast regions that may be included in each coarse node neighborhood at this level. See Figure 3.

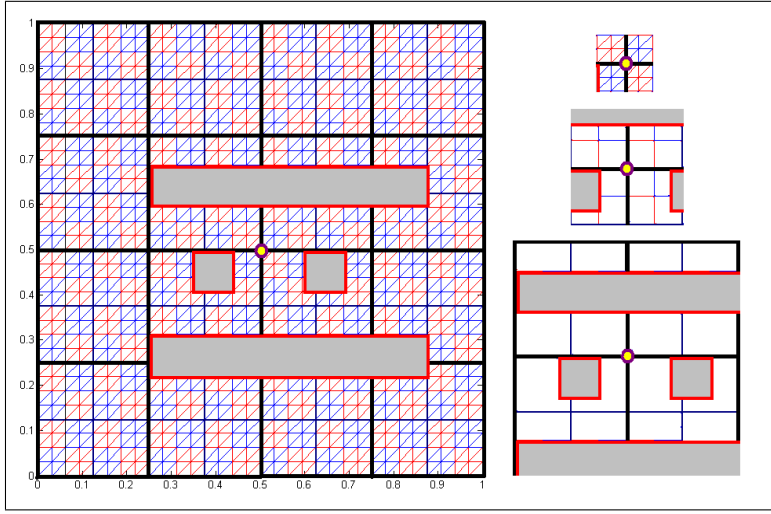


FIGURE 3. Right: Example of four nested triangulations $\mathcal{T}^{(0)} = \mathcal{T}_h$, $\mathcal{T}^{(1)} = \tilde{\mathcal{T}}_{\tilde{H}}$, $\mathcal{T}^{(2)} = \mathcal{T}_H$ and $\mathcal{T}^{(3)}$. Here $h = 1/32$, $\tilde{H} = 1/16$ and $H = 1/8$. Left: Example of the corresponding node neighborhood for the node $\mathbf{x} = (0.5, 0.5)$.

4.2.2. *Example of partition of identity using multiscale partition of unity.* Assume that the first level partition of identity is constructed using a piecewise (bi)linear partition of unity $\{\tilde{\chi}_j \in P^1(\tilde{\mathcal{T}}_{\tilde{H}})\}$. Introduce the multiscale partition of unity functions $\{\chi_i^{ms} \in P^1(\mathcal{T}_H)\}$. Function χ_i^{ms} is the $P^1(\mathcal{T}_H)$ approximation of the solution of

$$\begin{aligned} -\operatorname{div}(\kappa_{\tilde{K}}^{\tilde{H}} \nabla \chi^{ms}) &= 0 & \text{in } K \subset \tilde{\omega}_i \\ \chi^{ms} &= \chi^{lin} & \text{on } \partial K, \end{aligned}$$

where for every coarse element $\tilde{K} \in \tilde{\mathcal{T}}_{\tilde{H}}$

$$(4.13) \quad \kappa_{\tilde{K}}^{\tilde{H}} = \frac{\tilde{H}^2}{|\tilde{K}|} \sum_{x_r \in \tilde{K}} \sum_{\alpha=1}^{L_r} \int_{\tilde{K}} \kappa |\nabla w_{r,\alpha}|^2$$

is an up-scaled version of the fine scale coefficient κ . In this case, we can write

$$\chi_i^{ms} = \sum_s f_s^{(i)} \tilde{z}_{\tilde{x}_s},$$

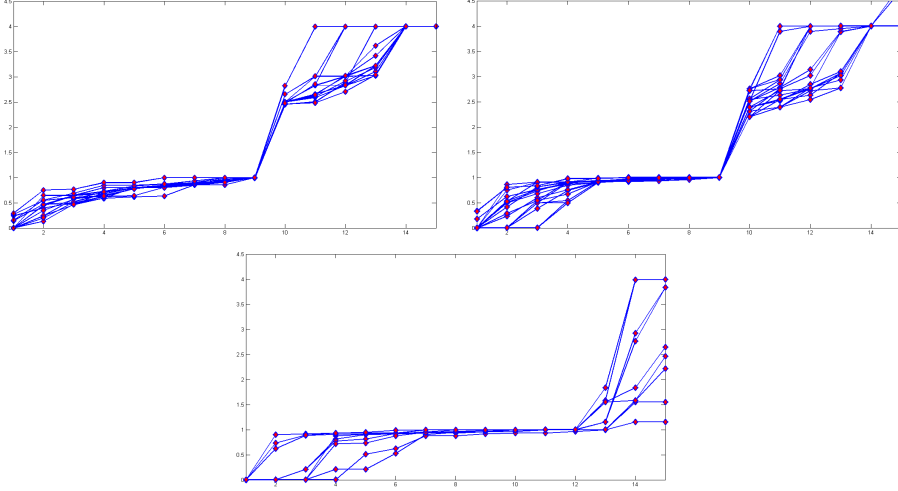


FIGURE 4. First 15 eigenvalues for all subdomains of $\mathcal{T}^{(1)} = \tilde{\mathcal{T}}_{\tilde{H}}$ (top left), $\mathcal{T}^{(2)} = \mathcal{T}_H$ (top right) and $\mathcal{T}^{(3)}$ (bottom). Each line plot represents the first 15 eigenvalues of one subdomain. Due to the scales of the figure, small eigenvalues appear on top of the horizontal axis. See Figure 3 for mesh and coefficient information.

where $\tilde{z}_{\tilde{x}_s} \in P^1(\mathcal{T}_H)$ is a usual nodal basis function. We use the functions $\{\chi_i \in \tilde{W}_{\tilde{H}}\}$ defined by

$$\chi_i = \sum_r \sum_{\alpha=1}^{L_r} \chi_{r,\alpha}^{(i)} w_{r,\alpha} \quad \text{where} \quad \chi_{r,\alpha}^{(i)} = f_r^{(i)},$$

and define $\{D^{(i)}\}$ as in (4.5). According to Remark 4.2, we can expect that this coarse space includes basis functions for each channels with respect to $\tilde{\mathcal{T}}_{\tilde{H}}$.

4.2.3. Optimal choice of partition of identity. The choice of the partition of identity should be done such that the variation introduced by all $D^{(i)}$'s in the high-contrast inclusions is minimal. Given a partition of identity $\{D^{(i)}\}$, the quotient for the eigenvalue problem (3.8) is

$$(4.14) \quad R_i(w; \{D^{(r)}\}) = R(w) = \frac{a_{\omega_i}(w, w)}{\bar{m}_{\omega_i}(w, w)},$$

where \bar{m}_{ω_i} is defined in (4.7) and depends on the partition of identity $\{D^{(i)}\}$. An optimal choice of the partition of identity $\{D^{(i)}\}$ is obtained when the number of small (asymptotically vanishing) eigenvalues is minimum for each coarse grid block. In this case, only degrees of freedom related to high-contrast channels will be added to the coarse space. We want to select partition of identity such that

$$(4.15) \quad \min_{\{D^{(r)}\}} \sum_{i=1}^N \sum_{\ell>1} \frac{1}{\lambda_{\ell}^{(\omega_i)}},$$

where the minimum is taken over all possible partitions of identity. A related more practical choice is given by the minimization problem

$$(4.16) \quad \min_{\{D^{(r)}\}} \sum_{i=1}^N \overline{m}_{\omega_i}(w_0, w_0)$$

or the quadratic minimization problem given by

$$(4.17) \quad \min_{\{D^{(r)}\}} \sum_{i=1}^N \int_{\omega_i} |D^{(i)} \omega_0|^2$$

where the minimum is taken over all possible partition of identity and $w_0 \in \widetilde{W}_{\widetilde{H}}$ is such that $\int_D \kappa |\nabla \omega_0|^2$ is bounded independent of the high contrast. Note that for partitions of identity defined as in (4.1) and $w_0 = 1$, the problem above can be viewed as the minimization problem corresponding to energy minimizing coarse basis functions in [18]. Similar procedures as in [18] can be implemented to approximate the solutions of such a minimization problem. The numerical solution of the minimization problem (4.17) is computationally expensive. Instead of the partition of identity chosen by solving the global problem (4.17) or (4.15), one can use locally defined functions with small energy. For instance, one can use multiscale basis functions that extend harmonically some prescribed boundary condition.

5. MULTIGRID METHODS

5.1. Notation and building tools. In this section, we extend our construction to the multilevel setting. We call recursively the construction and results from the previous section. Recall that we introduced a coarser mesh $\mathcal{T}^{(1)} \supset \mathcal{T}^{(0)}$ with parameter $h^{(1)}$. We assume that each coarse element $T_c \in \mathcal{T}^{(1)}$ is the union of fine elements τ with $\tau \in \mathcal{T}^{(0)}$. Define also the subdomains $\{T\}$ as coarse vertex neighborhoods. For each subdomain T , there is a coarse vertex x_T such that $T = \cup \{T_c : x_T \in T_c\}$. Each subdomain T contains only one coarse vertex x_T . Now, we define the subdomain matrices $A_{\mathcal{T}}^{(0)}$. For interior floating subdomains, let $A_{\mathcal{T}}^{(0)}$ be the finite element Neumann matrix corresponding to that subdomain. If T is a boundary subdomain, let $A_{\mathcal{T}}^{(0)}$ be the finite element matrix with homogeneous Neumann boundary conditions in the inner boundary $\partial T \cap D$ and homogeneous Dirichlet boundary conditions in the exterior boundary $\partial T \cap \partial D$. For any subdomain T , the matrix $A_{\mathcal{T}}^{(0)}$ can be obtained by local assembling of finite element matrices as f

$$A_T^{(0)} = \sum_{\tau \in T} I_{\tau}^{(0)} A_{\tau}^{(0)} I_{\tau}^{(0)T},$$

where $I_{\tau}^{(0)}$ is the extension by zero operator. Let $\{D_T^{(1)} : V^{(0)} \rightarrow V^{(0)}\}$ be a partition of identity; that is, $\sum_T I_T D_T^{(1)} I_T^T = Id$, where $Id : V^{(0)} \rightarrow V^{(0)}$ is the identity operator and I_T is the extension by zero operator.

Let $M_T^{(0)}$ be the matrix corresponding to the bilinear form \overline{m} ; that is,

$$M_T^{(0)} = \sum_{\tau \in T} I_{\tau}^{(0)} M_{\tau}^{(0)} I_{\tau}^{(0)T},$$

where $M_T^{(0)}$ is the local matrix corresponding to the (current level version of the) bilinear form \bar{m} defined in (3.6). See also (4.7). We solve the high-contrast eigenvalue problem

$$(5.1) \quad A_T^{(0)} \phi_k = \Lambda_k M_T^{(0)} \phi_k, \quad \phi_k = \phi_{k,T}, \quad \Lambda_1 \leq \Lambda_2 \dots \Lambda_k \leq \Lambda_{k+1} \leq \dots$$

This eigenvalue problem reveals the ‘‘small’’ part of the spectrum of the local subdomain matrix $A_T^{(0)}$. It can be shown that only a few small eigenvalues depend on the contrast, i.e., those few eigenvalues vanish asymptotically as the contrast increases. In particular, the number of these eigenvalues is related to the number of isolated high-conductivity inclusions and channels; see Section 3 for details. The idea is to include the corresponding eigenvector information into the coarse space. Let $L_T^{(0)}$ be an integer and define the coarse basis functions associated to the vertex x_T by

$$(5.2) \quad \Phi_k^{(1)} = D_T^{(1)} \phi_k^{(0)}, \quad k = 1, \dots, L_T, \quad \Phi_k^{(1)} = \Phi_{k,T}^{(1)}.$$

These are the coarse degrees of freedom. That is, we define the coarse space

$$V^{(1)} = \text{Span}\{\Phi_k^{(1)} = \Phi_{k,T}^{(1)}, \quad T \text{ subdomain}, \quad 1 \leq k \leq L_T^{(0)}\}.$$

Let $N_{T_c}^{(1)}$ be the number of coarse degrees of freedom in a coarse element, or coarse basis functions with the support containing a coarse element, $T_c \in \mathcal{T}^{(1)}$. With the (new) coarse basis functions, we construct local matrices $A_{T_c}^{(1)}$.

Denote by $P^{(1)}$ the matrix whose columns are the coarse basis functions defined including all subdomains T ; that is

$$P^{(1)} = [\Phi_{T,k}^{(1)}]_{T, 1 \leq k \leq L_T^{(0)}}.$$

The matrix $P^{(1)} : V^{(1)} \rightarrow V^{(0)}$ is the interpolation from the coarse space $V^{(1)}$. We use the Galerkin relation to define the coarse-level ‘‘1’’ matrix

$$A^{(1)} = P^{(1)T} A^{(0)} P^{(1)}.$$

We now consider the additional nested coarse meshes $\mathcal{T}^{(2)} \supset \dots \supset \mathcal{T}^{(\mathcal{L})}$ with parameters $h^{(2)}, \dots, h^{(\mathcal{L})}$, respectively. The procedure described above can be called recursively to construct coarse spaces $V^{(\ell)}$ and interpolations $P^{(\ell)} : V^{(\ell)} \rightarrow V^{(\ell-1)}$ (see Section 4.2). At level ℓ , we consider the coarser triangulation $\mathcal{T}^{(\ell+1)}$ and we proceed by constructing as before: local element matrices, $A_\tau^{(\ell)}, \tau \in \mathcal{T}^{(\ell)}$; subdomain local matrices, $A_T^{(\ell)}, M_T^{(\ell)}, T$ subdomain; coarse basis functions,

$$(5.3) \quad \Phi_k^{(\ell+1)} = D_T^{(\ell)} \phi_k^{(\ell)}, \quad k = 1, \dots, L_T^{(\ell)};$$

interpolation, $P^{(\ell+1)} = [\Phi_{T,k}^{(\ell)}]_{T,k}$; and coarse-level $\ell + 1$ matrix defined by

$$A^{(\ell+1)} = P^{(\ell+1)T} A^{(\ell)} P^{(\ell+1)}.$$

Here, $\{D_T^{(\ell+1)} : V^{(\ell)} \rightarrow V^{(\ell)}\}$ is a partition of identity of the ℓ th level degrees of freedom.

Note that $P^{(\ell+1)} : V^{(\ell+1)} \rightarrow V^{(\ell)}$ where we have defined the coarser space

$$V^{(\ell+1)} = \text{Span}\{\Phi_k^{(\ell)} = \Phi_{k,T}^{(\ell)}, \quad T \text{ subdomain}, \quad 1 \leq k \leq L_T^{(0)}\}.$$

Input: $x, b \in V^{(0)}$ and $A = A^{(0)}$. Output: $y = y_0 = MG(x, b)$.

- (1) Initialize: Set $y_0 = x$ and $r_0 = b - Ax$.
- (2) For $\ell = 0, \dots, \mathcal{L} - 1$, smooth:
 - (a) If $\ell > 0$, set $y_\ell = 0$.
 - (b) Perform additive Schwarz smoothing, i.e., for $s = 1, \dots, N_S$, compute

$$y_\ell \leftarrow y_\ell + I_{T_s}^{(\ell)} (A_{T_s}^{(\ell)})^{-1} I_{T_s}^{(\ell)T} (r_\ell - A^{(\ell)} y_\ell).$$

- (c) Compute the next level residual

$$r_{\ell+1} = P^{(\ell)T} (r_\ell - A^{(\ell)} y_\ell).$$

- (3) Coarse-grid correction: For $\ell = \mathcal{L}$, solve $A^{(\ell)} y_\ell = r_\ell$, i.e., compute

$$y_{\mathcal{L}} = (A^{(\mathcal{L})})^{-1} r_{\mathcal{L}}.$$

- (4) For $\ell = \mathcal{L} - 1, \dots, 0$, interpolate and post-smooth, i.e.,
 - (a) interpolate

$$y_\ell \leftarrow y_\ell + P^{(\ell)} y_{\ell+1}.$$

- (b) Post-smooth, i.e., for $s = N_S, \dots, 1$, compute

$$y_\ell \leftarrow y_\ell + I_{T_s}^{(\ell)} (A_{T_s}^{(\ell)})^{-1} I_{T_s}^{(\ell)T} (r_\ell - A^{(\ell)} y_\ell).$$

- (5) $MG(x, b) = y_0$.

FIGURE 5. Multigrid operator. Note that, in our construction, $P^{(\ell)} : V^{(\ell)} \rightarrow V^{(\ell-1)}$, $\ell = 1, \dots, \mathcal{L}$, and then, no information from the finest grid is needed to compute the correction at level ℓ .

Each eigenvalue problem is defined at a current level: $A_T^{(\ell)} \phi_k = \Lambda_k M_T^{(\ell)} \phi_k$. These are sparse small size eigenvalue problems. The corresponding spaces $V^{(\ell)}$ are nested; that is, $V^{(0)} \supset V^{(1)} \supset \dots \supset V^{(\mathcal{L})}$.

Observe that in [11], in order to construct new coarse basis functions, an interpolation of the solution of the local weighted eigenvalue problems into the finest space $V^{(0)}$ is needed in order to apply the partition of identity operator. In our paper, we use interpolations $P^{(\ell+1)} : V^{(\ell+1)} \rightarrow V^{(\ell)}$ constructed using partition of identity operators at each level. We need only previous level information to compute the tools needed at the current (coarser) level.

Now we describe the multigrid method. Given $x, b \in V^{(0)}$, we define $y = MG(x, b)$ as corresponding multigrid (V-cycle) operator with (multiplicative) Schwarz smoother with initial guess x and right-hand-side b . A detailed description of the computations is presented in Figure 5.1. The operator $r \rightarrow MG(0, r)$, $r \in V^{(0)}$, (as is well-known) is symmetric positive definite and can be used as a preconditioner.

5.2. Multilevel additive preconditioner (BPX). Now we define a BPX-like additive multilevel method with overlapping Schwarz method as smoother; see e.g., [17]. Given $r \in V^{(0)}$, we define

$$M_{add}^{-1}r = \sum_{\ell=0}^{\mathcal{L}} \sum_T P^{(\ell)} I_T^{(\ell)T} (A_T^{(\ell)})^{-1} I_T^{(\ell)} P^{(\ell)T} r,$$

where the second sum runs over all subdomains at level ℓ , $\ell = 0, \dots, \mathcal{L}$. See [5] for a two-level version of this method. In [5], it is proved for the two-level method that $\text{Cond}(M_{add}^{-1}A^{(0)}) \leq C(1 + \frac{1}{h^{(1)}\Lambda_{L+1}})$, where C is a constant independent of the contrast and $\Lambda_{L+1} = \min_T \Lambda_{L_T^{(1)}+1}$. If, in each subdomain, the right number of basis functions is chosen, then the previous estimate becomes *independent of the contrast*. We note that a naive multilevel extension of [5] would require the solution of fine triangulation eigenvalue problems in each subdomain at every level. In our construction in Section 5.1, we solve eigenvalue problems at the actual level and there is no need to visit the fine grid from the current coarse level.

5.3. A multilevel stable decomposition and condition number bound. Now we state the multilevel version of Lemma 3.2.

Lemma 5.1. *For every $v \in V^h = V^{(m)}$ there exist a decomposition*

$$v = \sum_{\ell=m}^{m+k_0} \sum_{i=1}^{N_S^{(\ell)}} v_i^{(\ell)}$$

and positive constants $C^{(\ell)}$, $\ell = m, m+1, \dots, m+k_0$ such that

$$\sum_{\ell=m}^{m+k_0} \sum_{i=1}^{N_S^{(\ell)}} a(v_i^{(\ell)}, v_i^{(\ell)}) \leq C_0^2 a(v, v)$$

with $C_0^2 = \prod_{\ell=m}^{m+k_0} C^{(\ell)}$. Moreover, there is a constant $C_{\mathcal{T}}$ depending only on the topology of the triangulations \mathcal{T}^{ℓ} , $\ell = m, m+1, \dots, m+k_0$ such that

$$C_0^2 \leq C_{\mathcal{T}}^{k_0} \left(\frac{1}{\Lambda_*} \right)^{k_0} \quad \text{where} \quad \Lambda_* = \min_{m \leq \ell \leq m+k_0} \max_{x_T \in \mathcal{T}^{(\ell)}} \Lambda_{L_T^{(\ell)}+1}.$$

We mention that the smallest *left out* eigenvalue Λ_* , depends on the bilinear partition of identity used (to define the bilinear form \overline{m} in (3.6) or (4.7) at each level). The idea is then, to select the partition of identity such that Λ_* is the biggest possible for a given coarse space dimension. See Section 4 for examples of construction of partition of identity functions. In general, Λ_* depends on the geometrical configuration of high-contrast regions (channels and inclusions).

Using the multilevel stable decomposition above, we can obtain bounds for the condition number of the multigrid method (5.1) and the multilevel additive preconditioner of Section 5.2. See [17, Chapter 5], [15] and references therein.

The above lemma implies level-dependent bounds of both additive (BPX) and (multiplicative) MG V-cycle methods given in the next Theorem.

Theorem 5.1. *We have the condition number bounds for the preconditioned operators: $\text{Cond}(MG(0, \cdot)A^{(0)}) \leq C_{MG}$ and $\text{Cond}(M_{add}^{-1}A^{(0)}) \leq C_{BPX}$, where the constants C_{MG} and C_{BPX} depend on the number of levels and on the contrast-independent eigenvalues $\Lambda_k = \Lambda_{k,T}^\ell$, $k \geq L_T$, T is a subdomain, $1 \leq \ell \leq \mathcal{L}$. In particular, for any V -cycle with k_0 -levels, we have $C \leq D \preceq C_0^2 \leq C_{\mathcal{T}}^{k_0} (1/\Lambda_*)^{k_0}$.*

5.4. AMLI-cycle MG: a recursive W-cycle like MG algorithm. According to Theorem 5.1 and Lemma 5.1, we see that the condition number is of the order of $C_{\mathcal{T}}^{k_0} (1/\Lambda_*)^{k_0}$, where k_0 corresponds to the number of levels. Then, the convergence rate of the preconditioned conjugate gradient will depend on the number of levels. In order to improve the performance of the multigrid method, we can stabilize the method in Figure 5.1 by using the more involved AMLI-cycle MG instead of V -cycle; see [17, Ch. 5]. Briefly explained, the AMLI-cycle MG, is a ν -fold recursive MG cycle with recursion applied at every level of multiplicity $k_0 \geq 1$, i.e., at levels $k = k_0, 2k_0, 3k_0, \dots$. Such cycle reduces to the well-known W -cycle for $\nu = 2$ and $k_0 = 1$.

The analysis in § 5.6.3, [17], gives that if ν , the number of recursive calls, is such that

$$\nu > C_{MG} = C^{k_0} \left(\frac{1}{\Lambda_*} \right)^{k_0},$$

the AMLI-cycle MG will provide a spectrally equivalent preconditioner with bounds independent of both the contrast and the number of levels used. However, we are also interested to keep the cost of applying the preconditioner under control, with the best cost being of order the number of fine-degrees of freedom. This gives an upper bound on ν , the number of recursive calls that we are allowed to use. Let n_k be the number of degrees of freedom at level k . Then, the analysis in § 5.6.3, [17], shows that if we can choose ν such that

$$(5.4) \quad \frac{n_k}{n_{k+k_0}} > \nu \geq C_{MG} = C^{k_0} \left(\frac{1}{\Lambda_*} \right)^{k_0},$$

we can guarantee both optimal complexity and uniformly bounded relative condition number of the AMLI-cycle MG preconditioner (both with respect to contrast and the number of levels).

If we assume certain growth in the number of the channels when we grow the coarse-element size from h_k to h_{k+1} , so that the number of channels grows like η^{d-1} , whereas the number of coarse vertices from level $k+1$ grows to fine-level k vertices like η^d , where $d = 2$ or $d = 3$ (for two or three dimensional domain D), and $1 < \eta \simeq \frac{h_{j+1}}{h_j}$ is the geometric coarsening factor, then it is easy to see that $\frac{n_k}{n_{k+1}} \simeq C\eta$. That is, due to the nature of long channels, they grow one dimension less than the volume growth of the elements (in all directions). Hence, we have

$$\frac{n_k}{n_{k+k_0}} \simeq (C\eta)^{k_0}.$$

To ensure (5.4), it is sufficient to choose $\eta > C \frac{1}{\Lambda_*}$. Note that we can choose η (it is a geometric coarsening factor) for any fixed Λ_* such that the above estimate (5.4) holds. It is clear though that all these estimates are asymptotic and apply for extremely fine meshes and highly channelized media resolved only by the finest mesh.

In our experiments, it appeared that even the V-cycle exhibits convergence factors bounded in terms of the levels.

6. COMPUTATIONAL COST OF THE METHODS

6.1. On the number of small contrast-dependent eigenvectors. As before, we assume that the coefficient κ is a simple function of high-contrast regions, channels $\{C_i\}$ and inclusions $\{I_i\}$

$$(6.1) \quad \kappa = 1_B + \sum_{i=1}^{N_{ch}} \eta_i^C 1_{C_i} + \sum_{i=1}^{N_{in}} \eta_i^I 1_{I_i}$$

Each subregion represents a high contrast inclusion (I_i) or channel (C_i). We assume that each high-contrast region is connected and has polygonal or smooth boundary. We also assume that each high-contrast region is the union of elements of the finest triangulation $\mathcal{T}^h = \mathcal{T}^{(0)}$. Assume that the classification in channels and inclusions above is made with respect to \mathcal{T}^j , for some j with $1 \leq j \leq \mathcal{L}$. Consider the partition of identity $\{D_i^{(j)}\}$ as constructed from multiscale finite element functions with linear boundary conditions. Recall the definition of \bar{m} defined in (4.7).

Consider the discrete generalized eigenvalue problem in a subdomain Ω ,

$$A\mathbf{q}_m = \Lambda M^{(j)}\mathbf{q}_m,$$

where the matrices A and $M^{(j)}$ are defined by

$$\mathbf{q}^T A \mathbf{p} = \int_{\Omega} \kappa \nabla p \cdot \nabla q \quad \mathbf{q}^T M^{(j)} \mathbf{p} = \bar{m}_{\Omega}(p, q).$$

It can be verified as in [5, 8] (see also [7]) that the number of small eigenvalues, asymptotically vanishing when the contrast increases, corresponds to the number of high-contrast regions where the associated degrees of freedom in the partition of identity $\{D_i^{(j)}\}$ vary considerably. See Lemma 4.1 and Remark 4.3. If the partition of identity is selected properly, then, the number of small asymptotically vanishing eigenvalues corresponds to the number of high-contrast channels with respect to $\mathcal{T}^{(j)}$ within the subdomain Ω . The previous statement implies that, if we take L_i equal to the number of channels with respect to $\mathcal{T}^{(j)}$ within the node neighborhood ω_i , then, we obtain a condition number independent of the contrast.

6.2. Preprocessing cost.

6.2.1. Triangulations and partitions. We do not assume that the grid is aligned with the coefficient in any way. Then, the preprocessing of the grid can be done at optimal cost independent of the coefficient.

6.2.2. On the solution of generalized symmetric eigenvalue problems. Given a subdomain Ω and the subdomain stiffness matrix A and mass matrix M , we need to solve the generalized symmetric eigenvalued problem $Az = \Lambda Mz$. This is a small sparse eigenvalue problem. There are several options for the numerical solution of this problem. We roughly describe the eigensolver in LAPACK; see [1].

Since M is positive definite, we can perform a Cholesky factorization, say $M = LL^T$. Then, we can make a substitution to get a standard eigenvalue problem of the form $L^{-1}AL^{-T}(L^Tz) = \Lambda(L^Tz)$ or $Cw = \Lambda w$, where $C = L^{-1}AL^{-T}$ and $w = L^Tz$. We note that, for general symmetric positive definite matrices, a Cholesky factorization can be performed in $O(\dim(A)^3/3)$ flops. Now, in order to solve the standard symmetric eigenvalue problem, matrix C is reduced to a Hessenberg tridiagonal form. This can be achieved in $4(\dim M_T)^3/3$ flops for general symmetric matrices. After a tridiagonal form is obtained, an iterative method for tridiagonal symmetric matrices can be used to compute the eigenvalues. For instance, we can apply an iterative QR algorithm. A QR factorization for tridiagonal matrices can be obtained in $O(\dim M_T)$ flops using, for instance, Givens rotations, [12]. The QR iteration to compute eigenvalues needs a QR factorization in each iteration.

At level ℓ , the total number of degrees of freedom in the subdomain Ω , according to the previous section, is given by,

$$(6.2) \quad \dim(A_{\omega_i}) = \sum_{\mathbf{x}_r^{(\ell-1)} \in \omega_i} L_r^{(\ell-1)}.$$

For instance, in Figure 1 the number of interior degrees of freedom (corresponding to the channels in the figure) is 14.

The generalized eigenvalue problem (3.7) uses the matrix $\widetilde{\widetilde{M}}_{\omega_i}$ obtained from the bilinear form \overline{m}_{ω_i} defined in (4.4). Assembling matrix $\widetilde{\widetilde{M}}_{\omega_i}$ involves the computation of the integrals in (4.4) for all chosen basis functions for all nodes neighboring the node i .

6.3. Online cost. In each iteration, we apply the multigrid operator described in Figure 5.1. This involves the solutions of local subdomain problems at every level. We mention that inexact solvers can also be used. An LU factorization is used in the numerical experiments presented in Section 7. At level ℓ and subdomain ω_i , the dimension of the linear system is given in (6.2). We note that the dimension of the local matrices A_{ω_i} are, in general, larger than the number of nodes interior to the subdomain ω_i (as is usual in classical multigrid methods). Then, the online cost of our methods is larger than the usual multigrid methods. The difference in cost will depend on the total number of extra degrees of freedom added. We recall that the maximum number of extra degrees of freedom that our methods yield for each node corresponds to the number of high-contrast regions on the subdomain corresponding to that node. An optimal choice of the bilinear form \overline{m} will reduce the number of extra degrees of freedom in each node, to the number of important channels in the corresponding subdomain.

Remark 6.1. *We recall that we are dealing with very ill-conditioned problems. Depending on the distributions of heterogeneities, the local problems at each level can be very ill-conditioned. This is due to the fact that if bounded energy basis functions cannot be achieved (here the choice of the bilinear form \overline{m} is important), the local matrix will be ill-conditioned with several scales of magnitudes in its entries. This will lead to very ill-conditioned local matrices. In this case, the procedures used to*

solve the local problems, have to be stable. Otherwise, the good performance of our methods can deteriorate due to the propagation of numerical errors.

7. NUMERICAL EXPERIMENTS

In this section, we present representative numerical experiments that show that the proposed methods have an optimal convergence in terms of contrast. We consider $D = [0, 1] \times [0, 1]$ and solve problem (2.1) with different distributions of high-contrast coefficients κ .

In the first experiment, we consider the coefficients depicted in Figure 6. We use Preconditioned Conjugate Gradient (PCG) with the preconditioners described above. The mesh and degrees of freedom information for the basis functions construction in Section 5.1 is displayed in Table 1. In this example, we use the bilinear form \bar{m} as defined in Section 4.2.1 and constructed using standard piecewise bilinear partition of unity. We have observed that Λ_{\min} (the smallest left out eigenvalue among all sub-domains) is independent of contrast in our simulations. In particular, the condition number of the preconditioned system using the multigrid operator as a preconditioner is 1.9 for contrasts $\eta = 10^5$ and $\eta = 10^7$ (the number of iterations is 9).

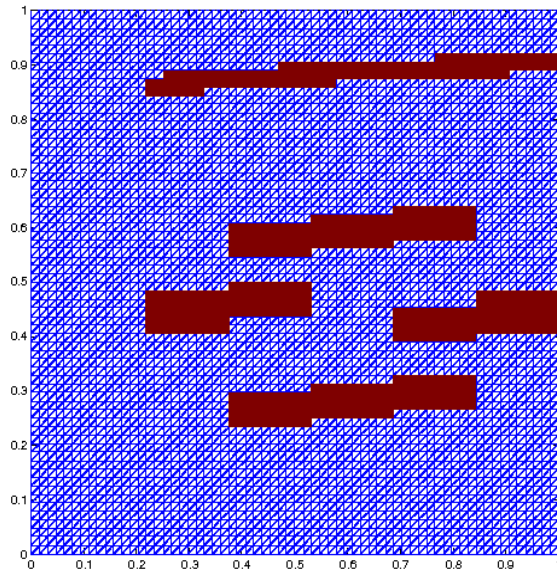


FIGURE 6. Coefficient corresponding to nine high-contrast channels. Red indicates the high-contrast part, $\kappa(x) = \eta$. White indicates value $\kappa(x) = 1$. The degrees of freedom information is in Table 1.

The previous examples consider a coefficient with long channels. Now we consider the example with coefficient depicted in Figure 7. This coefficient has channels and inclusions. The purpose of this second example is to show the importance of the choice of \bar{m} introduced in Section 4.2.2 (that uses multiscale partition of unity functions) in the final complexity of the methods. In this numerical test, we use a crude and inexpensive approximation of (4.13) and show that we can achieve some dimension

Level	h	Subdomains	nodes	xtra dof. 1	op	Λ_{\min}
0	1/64	32×32	4225	0(0)	1	
1	1/32	16×16	1089	0(0)	1.26	0.1538 (0.1538)
2	1/16	8×8	289	8(8)	1.33	0.2282(0.2282)
3	1/8	4×4	81	11(11)	1.35	0.2150(0.2149)
4	1/4	2×2	25	14(14)	1.36	0.1804(0.2734)

TABLE 1. Mesh, nodes, extra degrees of freedoms, minimum eigenvalue left out and operator complexity at each level for the coefficient depicted in Figure 6. See Section 5.1. The contrast values are 10^4 and 10^6 (in parenthesis).

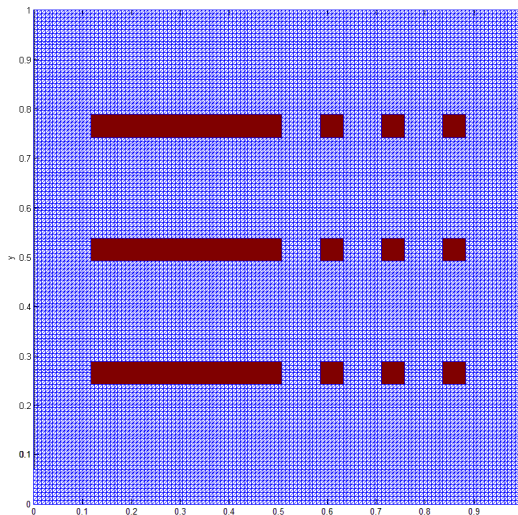


FIGURE 7. Fine mesh and coefficient corresponding to nine high-contrast channels and inclusions. Red indicates the high-contrast part, $\kappa(x) = \eta$. White indicates value $\kappa(x) = 1$. The degrees of freedom information is in Table 2.

reduction even with this approximation. We implement our multiscale partition of identity using a piecewise constant approximation of κ in each level. In Table 2, we present the resulting degrees of freedom information. We also report the extra degrees of freedom obtained if we use the bilinear form \bar{m} of Section 4.2.1 (that uses piecewise bilinear partition of unity). We see that the use of multiscale partition of unity function decreases the number of extra degrees of freedom needed for the construction. We mention that we are implementing simple procedures to select the number of small eigenvalues. In our implementation we keep all the eigenvalues less than a given threshold. As we stressed before, all the coarse level problems are ill conditioned in this case. Then, robust local solvers have to be used in this case.

Level	h	Subdomains	nodes	xtra dof.	Λ_{\min}
0	1/128	64×64	16641(16384)	0 (0)	
1	1/64	32×32	4225	0 (0)	0.1561 (0.1538)
2	1/32	16×16	1089	0 (0)	0.1904 (0.1680)
3	1/16	8×8	289	0 (0)	0.2230 (0.3828)
4	1/8	4×4	81	41 (55)	0.1009 (0.1258)
5	1/4	2×2	25	10 (36)	0.5231 (0.1848)
Level	h	Subdomains	nodes	xtra dof.	Λ_{\min}
4	1/8	4×4	81	43 (43)	0.1619 (0.1619)
5	1/4	2×2	25	69 (69)	0.1118 (0.1118)

TABLE 2. Mesh, nodes, extra degrees of freedoms, minimum eigenvalue left out at each level for the coefficient depicted in Figure 7. See Section 5.1. In the top table, we present the extra degrees of freedom when we use \bar{m} in Section 4.2.2 (that uses multiscale partition of unity). In the bottom table, we display the number of extra degrees of freedom if we use (an approximation of) \bar{m} in Section 4.2.1 (that uses piecewise bilinear partition of unity). The contrast values are 10^3 and 10^5 (in parenthesis).

The above results on the use of multiscale partition of identity are preliminary and show that we need a good choice of multiscale partition of identity to achieve a dimension reduction that is consistent with our theory. Multigrid numerical experiments using multiscale partition of identity are currently being designed. We are considering various choices for multiscale partition of identity that give small dimensional coarse spaces (including the ones presented here). We believe that one can achieve a substantial dimension reduction (within the genuine multilevel framework) for coarse spaces with careful choices of multiscale partition of identity and coarsening factors. This is subject of our current research and will be reported in future.

8. CONCLUSIONS

We develop and analyze multilevel methods for high-contrast problems. We present multilevel methods that use local generalized eigenvalue problems at the previous level to construct the coarse basis functions for the current level. The analysis presented here, extends to the genuine multilevel setting, the two-level domain decomposition preconditioners designed and analyzed in [5, 8, 11]. Our methods use a special bilinear form, \bar{m} , that enters in the local eigenvalue problems. This bilinear form \bar{m} is constructed using a partition of identity operator (that can be defined using partition of unity functions). The local eigenvalue problems identify the contrast-dependent modes that need to be included in the next coarser level solver to obtain contrast-independent performance. The choice of the bilinear form \bar{m} extends the idea of modified weight mass matrix introduced in [6, 8, 7]. It is also related to the abstract weighted Poincaré inequalities, [9, 10]. The methods presented here are constructed to target an optimal (w.r.t. physical parameters) multilevel stable decomposition; see also [9] for an abstract two-level setting. The stable decomposition is obtained in Theorem 5.1, where we prove that the relevant constants are independent of the

contrast of the coefficient. The multilevel decomposition, according to multigrid and multilevel analysis, gives condition number independent of the contrast. Our multilevel methods are designed to use Schwarz smoothers. We comment also on the complexity and computational cost of the proposed multilevel methods. We also discuss the theory behind the more involved (than the V-cycle) AMLI-cycle MG which can be used (if needed) to achieve level independent (in addition to contrast independent) bounds of the MG convergence. We present numerical results that support our analysis.

REFERENCES

- [1] Anderson, E., Z. Bai, C. Bischof, S. Blackford, J. Demmel, J. Dongarra, J. Du Croz, A. Greenbaum, S. Hammarling, A. McKenney, and D. Sorensen, *LAPACK User's Guide* (http://www.netlib.org/lapack/lug/lapack_lug.html), Third Edition, SIAM, Philadelphia, 1999.
- [2] M. Brezina, C. Heberton, J. Mandel, and P. Vaněk, *An iterative method with convergence rate chosen a priori*, UCD/CCM Report 140, April 1999. Available at <http://www-math.cudenver.edu/~jmandel/papers/>.
- [3] T. Chartier, R. Falgout, V. E. Henson, J. Jones, T. Manteuffel, S. McCormick, J. Ruge, and P. S. Vassilevski, *Spectral AMGe (ρ AMGe)*, SIAM J. Scientific Computing, 25(2003), pp. 1–26.
- [4] T. Chartier, R. Falgout, V. E. Henson, J. Jones, T. Manteuffel, S. McCormick, J. Ruge, and P. S. Vassilevski, *Spectral element agglomerate AMGe*, in Domain Decomposition Methods in Science and Engineering XVI, Lecture Notes in Computational Science and Engineering, Springer-Verlag, Berlin-Heidelberg, 55(2007), pp. 515–524.
- [5] Y. Efendiev and J. Galvis, *Domain Decomposition Preconditioners for Multiscale Flows in High-Contrast Media*, Multiscale Model. Simul. Volume 8, Issue 4, pp. 1461-1483 (2010).
- [6] Y. Efendiev and J. Galvis, *Domain Decomposition Preconditioners for Multiscale Flows in High Contrast Media. Reduced Dimension Coarse Spaces*, Multiscale Model. Simul. Volume 8, Issue 5, pp. 1621-1644 (2010).
- [7] Y. Efendiev and J. Galvis, *A domain decomposition preconditioner for multiscale high-contrast problems*, 19th International Conference on Domain Decomposition Methods, 2009.
- [8] Y. Efendiev and J. Galvis, *Coarse-Grid Multiscale Model Reduction Techniques for Flows in Heterogeneous Media and Applications*, Chapter of Numerical Analysis of Multiscale Problems, Lecture Notes in Computational Science and Engineering, Vol. 83.
- [9] Y. Efendiev, J. Galvis, R. Lazarov and J. Willems, *Robust domain decomposition preconditioners for abstract symmetric positive definite bilinear forms*, accepted.
- [10] Y. Efendiev, J. Galvis, R. Lazarov and J. Willems, *Robust Solvers for Symmetric Positive Definite Operators and Weighted Poincare Inequalities*, Submitted to Large-Scale Scientific Computing: 8th International Conference, LSSC 2011, Sozopol, Bulgaria.
- [11] Y. Efendiev, J. Galvis, and P. S. Vassilevski, *Spectral element agglomerate algebraic multigrid methods for elliptic problems with high-contrast coefficients*, 19th International Conference on Domain Decomposition Methods, 2009.
- [12] G. Golub and C. F. van Van Loan, *Matrix Computations*, Johns Hopkins Studies in Mathematical Sciences, 3rd Edition., Johns Hopkins University Press, Baltimore, MD, 1996.
- [13] I. G. Graham, P. O. Lechner, and R. Scheichl, *Domain decomposition for multiscale PDEs*, Numer. Math., 106(4):589-626, 2007.
- [14] I. Lashuk and P. S. Vassilevski, *On some versions of the element agglomeration AMGe methods*, Numerical Linear Algebra with Applications **15**(2008), pp. 595-620.
- [15] T. P. A. Mathew, *Domain decomposition methods for the numerical solution of partial differential equations*, volume 61 of Lecture Notes in Computational Science and Engineering. Springer-Verlag, Berlin, 2008.
- [16] A. Toselli and O. Widlund, *Domain Decomposition Methods - Algorithms and Theory*, Springer, Berlin, 2005.

- [17] P. S. Vassilevski, *Multilevel block-factorization preconditioners. Matrix-based analysis and algorithms for solving finite element equations*, Springer, New York, 2008.
- [18] J. Xu and L. Zikatanov, *On an energy minimizing basis for algebraic multigrid methods*, *Comput Visual Sci*, 7:121–127, 2004.

DEPARTMENT OF MATHEMATICS AND INSTITUTE FOR SCIENTIFIC COMPUTATIONS, TEXAS A&M UNIVERSITY, COLLEGE STATION, TX 77843-3368

E-mail address: efendiev@math.tamu.edu

DEPARTMENT OF MATHEMATICS AND INSTITUTE FOR SCIENTIFIC COMPUTATIONS, TEXAS A&M UNIVERSITY, COLLEGE STATION, TX 77843-3368

E-mail address: jugal@math.tamu.edu

CENTER FOR APPLIED SCIENTIFIC COMPUTING, LAWRENCE LIVERMORE NATIONAL LABORATORY, P.O. BOX 808, L-561, LIVERMORE, CA 94551, U.S.A.

E-mail address: panayot@llnl.gov